AD-A157 325 AN INVESTIGATION OF THE EFFECTS OF FUEL COMPOSITION ON COMBUSTION CHARACTERISTICS IN A T-63 COMBUSTOR(U) NAVAL POSTGRADUATE SCHOOL MONTEREY CA R W DUBEAU ET AL. 1/1

UNCLASSIFIED MAR 85 NPS67-85-004 F/G 21/4 NL

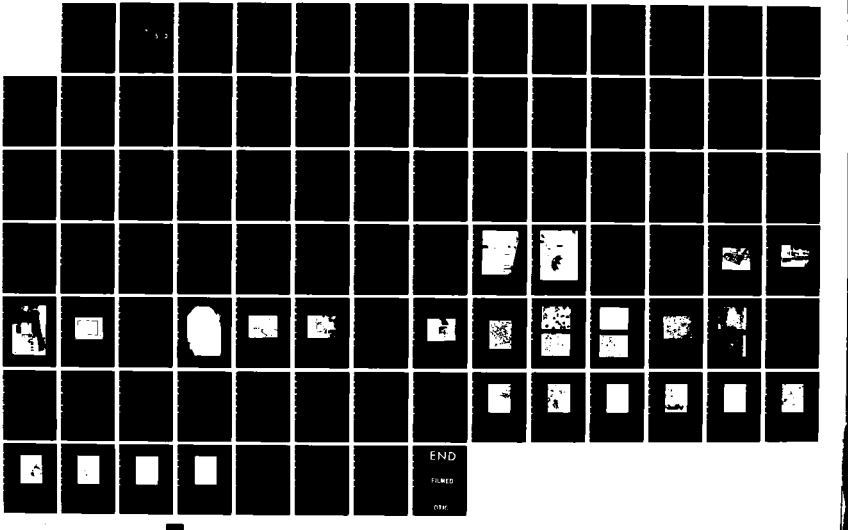

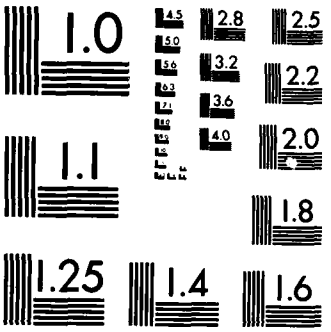

MICROCOPY RESOLUTION TEST CHART
NATIONAL BUREAU OF STANDARDS-1963-A

NPS67-85-004

NAVAL POSTGRADUATE SCHOOL

Monterey, California

AN INVESTIGATION OF THE EFFECTS OF FUEL COMPOSITION ON COMBUSTION CHARACTERISTICS IN A T-63 COMBUSTOR

R.W. Dubeau
P.J. Hickey
A.C. Krug
A.L. Lohman
J.P. Weller
D.W. Netzer

March 1985

Prepared for:

Naval Air Propulsion Center
Trenton, New Jersey 08600

NAVAL POSTGRADUATE SCHOOL
Monterey, California

Rear Admiral R. H. Shumaker
Superintendent

David A. Schrady
Provost

The work reported herein was supported by the Naval Air Propulsion Center, Trenton, New Jersey, as part of the Naval Environmental Protection Technology Program.

This report was prepared by:

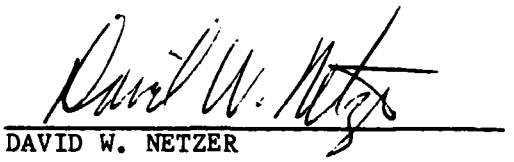

DAVID W. NETZER
Professor
Department of Aeronautics

Reviewed by:

M. F. PLATZER
Chairman
Department of Aeronautics

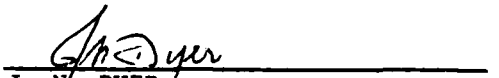

J. N. DYER
Dean of Science and Engineering

SECURITY CLASSIFICATION OF THIS PAGE (When Data Entered)

REPORT DOCUMENTATION PAGE		READ INSTRUCTIONS BEFORE COMPLETING FORM
1. REPORT NUMBER NPS67-85-004	2. GOVT ACCESSION NO. AD-A157 325	3. RECIPIENT'S CATALOG NUMBER
4. TITLE (and Subtitle) An Investigation of the Effects of Fuel Composition on Combustion Characteristics in a T-63 combustor		5. TYPE OF REPORT & PERIOD COVERED Progress October 1983 - March 1985 6. PERFORMING ORG. REPORT NUMBER NPS67-85-004
7. AUTHOR(s) R.W. Dubeau, P.J. Hickey, A.C. Krug A.L. Lohman, J.P. Weller, D.W. Netzer		8. CONTRACT OR GRANT NUMBER(s) N6237685WR00020
9. PERFORMING ORGANIZATION NAME AND ADDRESS Naval Postgraduate School Monterey, California 93943		10. PROGRAM ELEMENT, PROJECT, TASK AREA & WORK UNIT NUMBERS
11. CONTROLLING OFFICE NAME AND ADDRESS Naval Air Propulsion Center Trenton, New Jersey		12. REPORT DATE March 1985 13. NUMBER OF PAGES 88
14. MONITORING AGENCY NAME & ADDRESS(if different from Controlling Office)		15. SECURITY CLASS. (of this report) Unclassified 15a. DECLASSIFICATION/DOWNGRADING SCHEDULE

16. DISTRIBUTION STATEMENT (of this Report)

Approved for public release; distribution unlimited.

17. DISTRIBUTION STATEMENT (of the abstract entered in Block 20, if different from Report)

18. SUPPLEMENTARY NOTES

19. KEY WORDS (Continue on reverse side if necessary and identify by block number)

20. ABSTRACT (Continue on reverse side if necessary and identify by block number)

A T63 combustor was instrumented to allow measurement of centerline distributions of temperature and soot size and concentration using water-cooled probes. Three-wavelength light transmission measurements were also made at two locations to determine the mean soot size and NOx concentrations were measured in the exhaust duct. Five fuels of varying composition were used in the combustor and initial tests were conducted using two smoke-suppressant fuel additives.

DD FORM 1 JAN 73 1473 EDITION OF 1 NOV 65 IS OBSOLETE

S/N 0102-LF-014-6601

SECURITY CLASSIFICATION OF THIS PAGE (When Data Entered)

The data indicated that the aft region of the combustor contained a large, low temperature recirculation zone, surrounded by an annular region of higher temperature and lower soot concentration. Light transmission measurements appeared to yield reasonable particle size data when compared to collected samples. However, the extent of agglomeration in the collection probes was unknown.

Smoke-suppressant fuel additives were found to have reduced effectiveness in the present test series, apparently due to the unheated inlet air which was employed.

NO_x levels increased significantly with increasing combustor exhaust temperature (or fuel-air ratio). Soot concentration increased and transmittance decreased with increasing fuel-air ratio. The mean soot particle size was found to be between 0.21 and 0.26 microns, independent of fuel composition and fuel-air ratio.

TABLE OF CONTENTS

LIST OF TABLES

LIST OF FIGURES

NOMENCLATURE

A	PARTICLE CROSS-SECTIONAL AREA
C_m	PARTICLE MASS CONCENTRATION
d	PARTICLE DIAMETER
d_{32}	VOLUME-TO-SURFACE MEAN DIAMETER
f	FUEL-AIR RATIO
L	PATH LENGTH IN PARTICLE FLOW
$\dot{M}_a$	AIR MASS FLOW RATE
n	NUMBER CONCENTRATION OF PARTICLE
P_c	COMBUSTOR PRESSURE
Q	DIMENSIONLESS EXTINCTION COEFFICIENT
$\overline{Q}$	AVERAGE EXTINCTION COEFFICIENT
SEM	SCANNING ELECTRON MICROSCOPE
T	TRANSMITTANCE, TEMPERATURE
T_t	STAGNATION TEMPERATURE
λ	WAVELENGTH
ρ	PARTICLE DENSITY

SUBSCRIPTS

ex	COMBUSTOR EXHAUST DUCT
probe	WATER-COOLED SAMPLING PROBE
air	INLET AIR

I. INTRODUCTION

The maintenance requirements of high performance turbojet/turbofan engines require the Navy to utilize jet engine test cells at shore based jet engine rework facilities. The facilities provide a static, controlled environment in which to conduct engine overhaul evaluations prior to reinstallation aboard aircraft.

The Navy's use of jet engine test cells often must satisfy federal regulations issued by the Environmental Protection Agency (EPA). In addition, these minimum national pollution control guidelines are frequently made more stringent by local governmental regulations and controls. Currently, in California, the pollutants produced by engines while operating in shore based test cells must satisfy local requirements. Once installed in military aircraft, however, these engines are not required to conform to local regulations. Thus, the current primary concern is the test cell exhaust emissions which originate during engine post-overhaul testing. The solution desired is one which will allow the uninterrupted testing (i.e. without major and expensive overhaul of the existing test cells) throughout an engine's normal operating life while complying with all emission regulations.

Technology has not yet advanced to the point of being able to produce pollution-free, high-performance engines while still meeting demanding mission requirements and specifications. Therefore, another means of reducing pollutant levels is necessary. The options available, then, become clearly defined. Either the Navy must modify existing test cells to control the released pollution, or modify the fuel composition and/or combustion process to produce cleaner exhaust products. The first option is very expensive but is being accomplished on a limited basis at some facilities. Various research efforts have also been initiated to evaluate the effectiveness of fuel

additives as a relatively inexpensive solution to this problem. In recent years, many different smoke suppressant fuel additives have been developed. The Naval Air Propulsion Center (NAPC) has conducted evaluations of many of these additives in an effort to determine their relative effectiveness [Refs. 1 and 2]. The results of their testing indicated that metallic based additives, such as Ferrocene, were most effective in reducing test cell exhaust plume opacity. The difficulty with some metallic based additives, however, is that their low melting temperatures can cause a build-up of deposits in the turbine of high performance engines. Therefore, there is a need to find alternatives to such additives.

In answer to the need for both evaluating the effectiveness of the additives and understanding how they function to reduce opacity, a research program was initiated at the Naval Postgraduate School. A subscale test cell and a simulated gas turbine combustor were developed and refined until meaningful results could be achieved. Detailed description of the testing apparatus and data collecting techniques can be found in References 3 and 4.

The culmination of the research performed at the Naval Postgraduate School which was directed at smoke suppressant fuel additives and which used the original test apparatus was conducted by Bramer and Netzer [Ref. 4]. Six smoke suppressant fuel additives were tested in order to determine their effects on test cell stack exhaust gas opacity, volume to surface mean diameter of the particulate matter, exhaust particulate mass concentrations, and NOx concentrations. The additives ferrocene, DGT-2, and 12% Cerium Hex-Cem were found to be the most effective. The latter was significant in that cerium is a rare earth and has a higher melting temperature than iron. Additionally, it was found that the fuel additives that reduced stack opacity also reduced exhaust particulate mass concentration without

(3) to compare the particulate size data obtained using the sampling probe and the optical system. A series of three tests was conducted. The combustor was found to function satisfactorily during all tests conditions. A summary of the test conditions and data obtained are presented in Tables I and II. Test-to-test variation of the air flowrate was within 3%. Fuel flow rate control in these initial tests was determined from the pressure drop across the combustor fuel nozzle. Fuel tank pressure had to be accurately controlled. Subsequent tests employed a turbine flow meter to measure the flowrate and a throttling valve to control the flowrate.

TABLE I

EXPERIMENTAL CONDITIONS FOR INITIAL TESTS

Run #	Fuel Type	$\dot{m}_a$ (lbm/sec)	f	T_t probe (°R)	T_{exit} (°R)	P_c (psia)
1	Commercial JP-4	2.52	0.016	--	1572	99
2	NAPC-9	2.58	0.015	913	1580	100
3	NAPC-9	2.49	0.016	887	1683	98

IV. RESULTS AND DISCUSSION

A. INTRODUCTION

An initial series of tests was conducted to ensure proper functioning of the combustor, operating controls and diagnostic equipment. These tests used JP-4 and the combustor was operated at approximately 75% of normal rated conditions for the T-63 engine. The engine-centerline sampling probes were utilized only at the exit-end of the combustor. Soot samples were collected to evaluate the sampling-train and transmission measurements were made both within the combustor and at the engine exhaust. These tests were followed by apparatus modifications to improve system operation and data quality.

Subsequent test series were conducted in which the gas sampling and temperature probes were traversed along the engine axis from the aft location to the primary combustion region. In these tests several fuel types and additives were used.

After the final test series, the combustor was again removed from the stand to make further needed improvements.

The order of the presented results will follow the above discussion: (i) initial check-out tests, (ii) initial evaluation of the effects of fuel-composition and additives on emitted particulates and NOx concentrations and (iii) the latest modifications.

B. INITIAL CHECK-OUT TESTS

1. Introduction

The main purposes of this initial investigation were (1) to check for proper operation of the T-63 gas turbine combustor as modified for use in this test cell, (2) to evaluate the adequacy of the data collection equipment, and

Upon reaching steady-state transmittance for all three wavelengths, as well as steady NOx/NO levels and combustor exit gas temperature, the light source was extinguished. Steady-state transmittances were again obtained as combustion continued. Then the light source was reactivated and original steady-state conditions were re-established. If fuel additives were being tested, the pumps would then be activated singularly or together in order to observe any change in transmittance. Again the steady-state values with both the light on and off would be recorded. Upon shutdown, zero and 100% transmittance values were rechecked.

If a temperature profile was being obtained, the traversing mechanism was activated. It took approximately thirty seconds for the probe to move the length of the combustor. If a particulate sample was being taken, isokinetic conditions had to first be established using the restrictor valve in the sampling line. Then the sample actuating switch was activated. Sample collection lasted thirty seconds, at the end of which the sampling switch was turned off. Isokinetic conditions were monitored and maintained for the duration of the sample collection.

After data collection was completed the fuel was turned off to terminate the run. The main air switch was left on for a few seconds to clear the combustor of any residual fuel and to help cool the equipment. If a particulate sample had been taken, the filter papers were removed from their holders and placed in a dessicator. The filters were subsequently weighed, then trimmed and mounted on SEM stems to be photographed.

III. EXPERIMENTAL PROCEDURE

A. EQUIPMENT SET-UP

In order to achieve a consistent test environment, all necessary equipment was allowed a nominal warm-up period of 30 minutes. This included all electronic recording devices (strip chart recorders), thermocouples, the optical system (projector, photodiodes, voltage surge surpressor), and the NOx analyzer. During this warm-up cycle, main air supply valves, fuel tank pressurization lines and valves, and control panel nitrogen control valves were cycled. Pressure transducers were calibrated using a dead weight tester.

Following system warm-up, optics were checked for proper alignment and detector voltage output. Also, zero and 100% transmittance readings were taken at this time with the light source off and on respectively. "Set" values for air and fuel line pressures were then adjusted to desired levels using hand loading valves at the control panel.

When obtaining axial temperature profiles, the power supply to the linear potentiometer was also turned on. For particulate collection runs the filtering paper was weighed and put in place, then the oven and heated gas sampling hose were turned on.

B. TEST RUN

Readings were obtained for 100% transmittance with air flow in order to account for any opacity due solely to particulates in the dry air. Then the igniter and fuel switches were activated simultaneously to complete the light-off. Immediately upon light-off the operator could monitor and adjust fuel flow via digital readout and a throttling valve.

Probe travel was managed with a metering valve which controlled the rate of nitrogen flow to the pneumatic actuator. Particulate sampling was controlled by a single control which diverted flow through the sampling filters and activated the sampling timer. A restrictor valve in the sampling line was used to establish and maintain isokinetic conditions. Stagnation pressure in the air supply line and pressure in the combustion chamber were recorded on a Visicorder. Stagnation temperature in the air supply line and in the exhaust chamber were recorded on strip charts. Axial temperature profiles were made on an X-Y plotter. Records of the particulate samples were simply the SEM photographs.

For the purposes of this investigation, the optical transmission data were recorded using three strip chart recorders. The outputs of the optical systems were directly attached to the recorders to provide permanent, real time recording of the transmissivity within the combustor and at the engine exhaust. In future testing, the data acquisition and processing will be accomplished by an existing computer based data acquisition and processing system. Samples of the combustion particulate matter were controlled by the extractive probe system and analyzed using a SEM.

G. NITROGEN OXIDES ANALYZER

A monitor Labs model 8440E analyzer (Figure 14), which is a gas phase chemiluminescence detection device, was utilized with a strip chart recorder to provide real-time permanent traces of both NOx and NO concentrations. NO_2 (nitrogen dioxide) could be calculated simply as the difference between NOx and NO.

The remainder of the system consisted of a heated sample line (Technical Heater Inc., model LP212) leading from the probe to an oven (Figure 12). The line was heated to prevent condensation. The oven, heated to 80° centigrade, contained a two stage filter utilizing 47 mm diameter Nuclepore membrane filters: 8μm pore size for the primary filter and 0.2μm pore size for the secondary. Nuclepore filters were chosen for their adaptability for viewing with a scanning electron microscope (SEM). A schematic of the initial extractive probe sampling system is shown in Figure 13 [adapted from Ref. 9]. Subsequent testing was conducted without utilization of the vacuum pump in the collection line. Motor pressure was more than adequate to provide the required isokinetic flow conditions.

The stagnation thermocouple probe was built to the same outer dimensions as that of the extractive probe. A chromel-alumel thermocouple was utilized during the initial testing and was placed along the centerline of the probe. The purpose of this apparatus was to provide an axial temperature profile for each test. The thermocouple probe was mounted in the same location as the extractive sampling probe.

F. CONTROLS AND DATA RECORDING

The entire test sequence was conducted from the control room. The fuel system included a control valve and pressure gage for setting nitrogen pressure in the tank, and a vent switch for relieving pressure. A fuel shut-off switch was located next to the ignitor switch on the main control panel. Above the control panel was a throttling valve for adjusting the fuel flow. On the air supply there was a control valve for adjusting the pressure supplied to the sonic nozzle and a switch to open and shut the air supply electronically.

Using three transmittance ratios, three values of d_{32} were obtained. If all three d_{32} values were not nearly identical, the complex refractive index and/or the standard deviation chosen were not correct. m and T values were varied until all three values of d_{32} were nearly identical. Once $\overline{Q}_\lambda$, d_{32}, and and T_λ were known, mass concentration could be calculated with the following rearrangement of equation (6):

$$C_m = -\frac{2}{3}\frac{[\rho d_{32}]}{\overline{Q}_\lambda L}\ln T_\lambda \qquad (8)$$

E. EXTRACTIVE AND THERMOCOUPLE PROBE SAMPLING SYSTEMS

The extractive sampling probe used in this investigation and the associated sampling system were adapted from the design used by Samuelson, et. al. [Ref. 9]. The probe was constructed of stainless steel and was water cooled. Included in the probe design were two isokinetic pressure ports, the primary particulate sampling line, a gas sampling port, and an inert gas injection port. The isokinetic pressure ports were connected to a pressure transducer and monitored to insure that the gas velocity entering the probe was nearly identical to that in the combustor. A schematic of the probe is shown in Figure 9. A photograph of the probe is presented in Figure 10.

The probe holder had two linear bearings which allowed for linear motion along the combustor axis (Fig. 11).

Motion was achieved by pushing the probe holder with a remotely controlled, pneumatically driven rod. A pneumatic actuator was fixed to the test stand. A linear potentiometer was connected to the probe holder to provide a voltage proportional to probe displacement.

beam traverses, (C_m) is the mass concentration of particles, (ρ) is the density of an individual particle, and (d) is the particle diameter.

A more useful relationship was developed by Dobbins [Ref. 8] to allow for a distribution of particle sizes:

$$T = \exp\ [-(3\overline{Q}C_m L/2\rho d_{32})] \tag{5}$$

where ($\overline{Q}$) is an average extinction coefficient and (d_{32}) is the volume-to-surface mean particle diameter. Taking the natural logarithm of equation (5) and writing it for a specific wavelength of light:

$$\ln\ [T_\lambda] = \overline{Q}_\lambda\ [-3C_m L/2\rho d_{32}] \tag{6}$$

Assuming Cm, L, ρ, and d_{32} remain constant, the ratio of the natural logs of the transmittances for two wavelengths of light is:

$$\frac{\ln\ [T_{\lambda 1}]}{\ln\ [T_{\lambda 2}]} = \frac{\overline{Q}_{\lambda 1}}{\overline{Q}_{\lambda 2}} \tag{7}$$

A Mie scattering computer program, provided by K. L. Cashdollar of the Pittsburgh Mining and Safety Research Center, Bureau of Mines, produced calculations of $\overline{Q}_\lambda$ and the $\overline{Q}_\lambda$ ratios as a function of d_{32}. The program required as inputs the complex refractive index of the particles, the refractive index of the surrounding medium, the standard deviation of the particle distribution and the wavelengths of light. Most of the particulates aft of the primary combustion zone can be reasonably assumed to be carbon. The following values were utilized in this investigation:

Complex Refractive Index of Particles (m = 1.95 - .66i), (m = 1.9 - .35i) (m = 1.80 - .30i), and (m = 1.60 - .60i).

Refractive Index of Surrounding Medium (1.0 for air).

Standard Deviation of the Distribution (σ = 1.5, 2.0).

The transmitted light exiting the combustor viewport entered a 10 inch long, 0.25 inch diameter, blackened tube which minimized detection of forward scattered light. To enhance the linearity of the diode outputs at all wavelengths, and to prevent detector saturation, the rear of the tube was reduced in size using a small orifice, 0.10 inch in diameter. Upon exiting the tube, the light passed through two beam splitters which redirected the three resulting beams to photodiodes via narrow pass filters. In the initial tests wavelengths of 1.014, .650 and .5145 microns were used. Later tests utilized wavelengths of .850, .650, and .466 microns. These particular values were selected in an attempt to minimize the effects of combustor generated light and to provide a spread in the wavelengths for accuracy in determining mean particle sizes.

The light source/detector pairs were designed to measure the fraction of light transmitted through the combustion products (the transmissivity). This value is determined by comparing the photodiode output without particles present to that with particles present. The voltage output of each photodiode was continuously recorded on a strip chart recorder.

K. L. Cashdollar [Ref. 7] successfully applied Mie scattering theory to the measurement of soot particle size and concentration in a cloud of smoke. Bouguer's law [Ref. 7] for the transmission of light through a cloud of uniform particles can be written:

$$T = \exp(-QAnL) = \exp[-(3QC_mL/2\rho d)] \qquad (4)$$

where (T) is the fraction of light transmitted, (Q) is the dimensionless extinction coefficient, (A) is the cross sectional area of particle, (n) is the number concentration of the particles, (L) is the path length the light

unit, and a signal conditioner/display unit. The light source and the detector unit were mounted across the exhaust stream to provide a read-out of exhaust stream opacity. The unit is shown installed in Figure 1.

D. OPTICAL DETECTOR SYSTEM FOR DETERMINATION OF PARTICLE SIZE

Light transmission and detection techniques utilized during the studies conducted on the subscale turbojet test cell were adopted for use in this investigation. Non-intrusive data collection techniques were considered preferable to extractive probe data collection because the flow conditions within the combustor would remain undisturbed. In an effort to accomplish this non-intrusive data collection, the collimated white light sources and detectors used by Thornburg, Bramer, and Netzer [Refs. 3,4] were positioned to make measurements within the combustor, near the combustor exit. In the initial tests, a second, identical system was located to make measurements within the exhaust stream from the test apparatus.

The apparatus consisted of the following components, mounted on free-standing tables:

1. A projector with a 750 watt incandescent bulb to provide the white light source (Fig. 7). Uniform intensity light was provided by placing a piece of diffuse glass between the lamp and projector lens.

2. A beam collimation system consisted of a 0.04 inch diameter pinhole and a 31.5 mm (diameter) achromatic lens with an 80 mm focal length (Figure 7).

3. Viewports located on either side of the combustor in the most rearward position possible along the combustor centerline.

4. A detector box containing the three wavelength narrow-pass filters and photodiodes (Figure 8).

of the modified combustor is shown in Figure 3.

Air was supplied to the combustor from a 3000 psi reservoir. At this pressure, the reservoir could provide nearly fifteen minutes of run time. A schematic of the air and fuel supply systems is shown in Fig. 4. The air feed line was fitted with a dome pressure regulator and a sonically chocked nozzle to provide the desired flow rate during engine operation.

Other subsystem components included a fuel supply system, an instrumentation package, various optical transmission measurement systems, and a water cooled sampling probe system. These items will be fully described below.

B. FUEL SUPPLY SYSTEM

Fuel flow was provided by a nitrogen-pressurized, 20 gallon tank. Fuel flow rate to the electrically controlled solenoid valve and fuel nozzle was measured with a turbine flowmeter located just upstream of the additive injection point in the fuel line (Fig. 4). Fuel flow rate could be controlled from 0.00 to 0.50 gallons-per-minute (0.005 gpm) using a hand-operated throttle valve and a digital flow-rate indicator located at the main control panel (Fig. 5). Additionally, two Eldex (model E) precision metering pumps (Figure 6) were located downstream of the turbine flowmeter to control fuel additive flowrates. Proper additive and fuel mixing was accomplished with a swirl-type mixer. Additive flow rate could be controlled between 0.2 and 5.0 ml per minute. Actuation via separate pump switches was performed at the main control panel.

C. TRANSMISSOMETER

The transmissonmeter utilized during this study was a Leads and Northrop model 6597. The transmissometer consisted of a white light source, a detector

II. EXPERIMENTAL APPARATUS

A. TEST CELL AND COMBUSTOR

The primary test article used in this experiment was a gas turbine combustor (T63) mounted on a test stand (Figures 1 and 2). The T63-A-5A engine was built by Allison Detroit Diesel and is utilized in several operational aircraft, most notably, the Army OH-6A helicopter. The combustor incorporated in this engine possessed several unique characteristics which made it attractive for use in the present investigation.

The combustion system was of singular chamber, reverse flow design. The single chamber feature was convenient because the entire combustion system could be mounted and studied, a more preferable option than attempting to mount only a portion of the popular annular, or multiple chamber designs. The reverse flow feature greatly simplified the mounting of optical detection windows and supplied a buffer region of cooler, cleaner air between the viewing windows and the primary combustion zone. Furthermore, the take-off rated air flow of this engine is 3.2 lb/sec, and this relatively small air flow rate fit nicely with the existing high pressure air supply system at the Combustion Research Laboratory. A larger air flow rate would have severely limited the run time for each experiment.

The exhaust gases produced in the combustor exited through a fixed area turbine nozzle block. Subsequently, they entered a locally manufactured aft closure and (initially) variable area exhaust nozzle. The initially employed exhaust nozzle exit apertures (Figure 2) could be manually varied to supply the necessary back pressure for the combustor. Without such a device, the pressure drop across the combustor liner could have caused failure of the liner. Subsequently, exhaust pipes were welded to these holes to direct the exhaust flow away from the probe holder/traversing mechanism. A schematic

a) decreased engine smoke number at high power settings

b) no significant changes in oxides of nitrogen emissions.

2) Increased fuel aromatic content contributed to:

a) increased engine smoke number at high power settings

b) no significant changes in oxides of nitrogen emissions.

3) Increased operating temperature (which was a linear function of fuel flow and engine power) contributed to:

a) increased oxides of nitrogen

b) increased engine smoke number.

To obtain a better understanding of the ways in which fuel composition and additives affect the combustion process requires the use of a well-instrumented, modern gas turbine combustor. Even then, data are difficult to obtain which can be used to determine the mechanics of soot formation, agglomeration and consumption within, and exterior to, the combustor.

At the Naval Postgraduate School a new test facility has been constructed to permit the study of the effects of fuel composition and fuel additives on the sooting characteristics within and exterior to the combustor. The new facility incorporates a full size engine combustor (T63) which can be operated at more realistic pressure levels than the original apparatus.

This report discusses the test facility and instrumentation, and initial results obtained on the effects of fuel composition on exhaust pollutants. The results of this initial study pointed out the need for further system and diagnostic technique improvements. These improvements, which are currently being made, are also discussed.

reducing average particle diameter. Finally, NOx concentration at the test cell stack exhaust was not significantly changed by any of the fuel additives tested.

While the results obtained from this research were significant and provided much needed information on the capabilities and limitations of different smoke suppressant fuel additives, it was clear that additional research was necessary due to the need to clarify the mechanisms by which the additives worked and due to the constraints imposed by the testing apparatus. In addition to the use of additives, alternate, or wider specification fuels are being considered. These fuels may not only effect exhaust emissions and engine life, they may be required in the future as current oil reserves are depleted.

Recently the Air Force Aero Propulsion Laboratory has conducted research into the effects of broad variations in fuel properties on the main combustor and turbine systems of various turbojet and turbofan engines [Ref. 5]. The study concerned itself predominantly with the effects of fuel chemical composition and physical properties on engine operability and durability. The effects on exhaust gas emissions were also reported. Fuel hydrogen content was found to be the dominant variable that affected combustion properties, and was used to correlate smoke and NO_x emissions data.

Alternate fuels have also been recently evaluated at the Naval Air Propulsion Center (NAPC)(Ref. 6). Using an Allison T63-A-5A engine, NAPC designed their tests to investigate the effects of fuel properties on engine exhaust emissions levels and engine performance. Some of their findings are listed below.

1) Increased fuel hydrogen content contributed to:

TABLE II

EXHAUST GAS OPACITY, TRANSMITTANCE VALUES, AND EXTINCTION COEFFICIENT RATIOS FOR INITIAL TESTS

Run Number	Exhaust Opacity (%)	WITHIN COMBUSTOR T_λ .5145	WITHIN COMBUSTOR T_λ .650	WITHIN COMBUSTOR $\frac{\bar{Q}_{.650}}{\bar{Q}_{.5145}}$	ENGINE EXHAUST T_λ .450	ENGINE EXHAUST T_λ .650	ENGINE EXHAUST T_λ 1.014
1	7.3	.40	.57	.61	.98	.99	.96
2	7.0	.40	.68	.42	.98	.98	.99
3	7.0	.37	.70	.36	.99	.99	.98

2. Sampling Probe

The extractive probe sampling system used during this investigation was adapted from the design used by Samuelsen, et. al. [Ref. 9]. While this water cooled probe design proved sufficient for Samuelsen's purposes, it was unknown whether or not it would survive the T-63 combustor environment which was operated at higher pressures. The purpose of these tests was to determine if the sampling probe could survive the new environment, and if a representative particulate sample could be obtained with the Nuclepore filter system. For these initial tests, a water heater was not employed for the probe cooling water.

The extractive probe was placed in the combustor so that the head of the probe was at the rear of the combustion chamber. This insured that the probe was well clear of the primary combustion zone, and that the least severe conditions possible were experienced by the probe during these initial tests. After the combustor was running at steady state conditions and isokinetic conditions were achieved, a sample was taken for four minutes.

SEM photographs were taken of both sampling filters. Two different preparations were employed, gold coating and aluminum coating, as indicated on the photographs. In addition, two different SEM's were utilized: a Cambridge S4-10 and a Hitachi S540. Both SEM's and both coating methods produced similar results. Figure 15 is a relatively low magnification photograph of the primary filter (8μm). This figure shows a number of large agglomerations. Figures 16a and b show that these structures are puff like in nature and significantly larger (30μm to 50μm) than the pore size of the filter. These observations were not totally unexpected, based on the results of Samuelsen et. al. [Ref. 9].

The sample rates of this experiment were significantly higher than those of Samuelsen ($\bar{V}\cong 22$ mps vs. 15 mps). Also, N_2 dilution was not used during these initial tests. At higher magnifications (Figure 17a and b), smaller agglomerates of particulate matter can be seen between the larger puff like structures.

The sample collected by the secondary filter (.2μm), can be seen in Figures 18 and 19. In Figure 18, it should be observed that the filter is virtually saturated by the sample. A higher magnification (Figure 19a and b), however, revealed that some individual particles could be observed. At a magnification of 40,000, the few individual round particles observed had diameters between .08 and .15 μm.

The extractive probe sample results raised several questions. First, were the puff like structures on the primary filter actually present in similar form within the combustion chamber or were they probe collection induced agglomerations of the smaller particles? Second, what effects would occur from heating the cooling water and/or using dilution (N_2) [per Ref. 9]. Finally, what effects would result from decreasing the sample time?

It is obvious that the sample time used for these initial test was too great. Both filters were saturated with sample matter to the point of restricting the sample flow. The flow restriction was observed to begin at approximately 30 seconds of sample time. After this time, isokinetic conditions were impossible to achieve. The quantity of sample matter collected made quantitative analysis of the sample difficult. In addition, the nature of the sampling system (i.e. - bends in the sample line, etc.) will cause some agglomerates to form from individual particles.

3. Optical Measurements

As discussed earlier, the primary purpose of the collimated white light sources and the three-wavelength light detection units was to optically determine the size and concentration of the particulate matter. This was to be done at a position inside the combustion chamber, as well as at the engine exhaust. The opacity of the engine exhaust was also monitored continuously throughout the run.

The optical data extracted during each of the three runs are presented in Table II. It was not possible in these initials tests to determine d_{32} or C_m from the transmissivities provided by the optical equipment.

The white light transmissometer located at the engine exhaust provided a fairly consistent opacity reading of approximately 7% throughout the test runs. The transmissometer was large enough in cross-section to capture a representative sample of exhaust gases. This opacity is quite small and indicated that the engine burned extremely clean under the present test conditions.

In the same manner as the transmissometer, the three frequency light detector at the exhaust gave consistently high readings of transmissivity. However, the small collimated beam passed through only a very small section of the stratified exhaust stream. Because the transmissivities were all very high, the extinction coefficient ratios could not be accurately determined. Small changes in high transmittance values greatly effect the log ratios. In other words, the sensitivity of the optical technique used at the exhaust was insufficient for use with such a clean burning test condition. To obtain meaningful data at the exhaust, the combustor must either be run with higher exhaust gas opacity (i.e., a more fuel rich setting), or more of the exhaust gases must be directed past the light detection equipment. Light scattering measurements may be successful at these high transmittance values.

Problems of a different nature were experienced with the optical unit located in the combustor. During a preliminary run on the engine, it was discovered that two of the wavelengths used (i.e., .450 and 1.014 microns) were saturated by light produced by the combustion process. For subsequent test runs, the .450 micron filter was replaced with a .5145 micron narrow pass filter. Both the .5145 and the .650 micron wavelengths produced good transmissivity data (Table II). The problem, however, resulted from the closeness of the two wavelengths and the elimination of the data from the third wavelength. The extinction coefficient ratios produced from the transmissivity data (Table II) were consistently below the theoretical Mie scattering curves. Because the two wavelengths were so close, the accuracy of the transmittance ratios also suffered. Therefore, it was apparent that, for future testing, three new frequencies had to be selected or a means to eliminate the combustion generated light had to be incorporated.

4. Temperature Measurements

The water cooled stagnation temperature probe was placed at the rear end of the combustor on the centerline. The combustor exhaust actually occurs in an annulus at its outer diameter. This apparently results in a large recirculation zone in the central region with a significantly lower temperature. The temperature measured in this region using the probe was approximately 600 °F lower than the temperature measured in the downstream exhaust ducting.

The low values of transmittance in the aft region of the combustor (Table II) compared to the engine exhaust opacity also indicated that this region contained large quantities of soot.

5. Conclusions and Recommendations from Initial Tests

(a) The T-63 combustor operated reliably.

(b) Improved control of the fuel flow rate was required.

(c) Engine exhaust opacities were too low (at the location utilized) to permit reliable use of the 3-wavelength transmission measurement apparatus. The traverse should be made further upstream where the gas flow is uniformly distributed.

(d) Particulate sampling time along the engine centerline should be reduced to less than 30 seconds. Heated cooling water and/or N_2 quenching may help to reduce the observed agglomeration.

(e) Light transmission measurements within the combustor were hampered by the presence of a relatively cool recirculation zone at the aft end of the combustor and by significant combustor radiation across the visible spectrum.

C. INITIAL PARAMETRIC INVESTIGATION OF THE EFFECTS OF FUEL COMPOSITION ON SOOT AND NOX EMISSIONS.

1. Introduction

The purpose of this part of the investigation was to initiate a study of the effects of varying fuel composition, operating characteristics, and fuel additives on the production, consumption, and general behavior of soot and NO_x emissions. This was to be accomplished by using different fuel compositions (supplied by NAPC) and several previously tested smoke suppressant fuel additives in the T63 combustor. Engine centerline profiles of temperature and soot characteristics were to be determined by using water cooled probes and optical measurements. The ultimate goal is to use this type of data to help delineate the expected behavior of proposed new additives and fuel compositions.

Some data already exist for the T63 engine from tests conducted at NAPC [Ref. 6]. Those data were used for comparison with the data obtained in the present investigation.

A careful selection of detector wavelength was made in order to minimize the effects of combustor generated light on the transmittance measurements. Electronic low-pass filters were also applied for similar reasons to the visible and IR signals. Exact alignment of the collimated light source and the detector apparatus appeared to be the most crucial factor affecting the reliability of results. Therefore, careful alignment was performed before a test run with zero and 100% transmittances recorded both before and after the run. In addition to the improved optical detection apparatus, a turbine flow meter was installed to enhance monitoring and control of the fuel flow and combustor exhaust temperature.

The fuels used in this investigation were provided by the Naval Air Propulsion Center (NAPC). Fuel compositions are detailed in Ref. 6, and summarized in Table III.

2. Fuel Composition and Additive Effects Determined from Light Transmission Measurements

Despite initial plans to screen all ten of the fuels obtained from NAPC, only five fuels were actually tested. These included the two fuels which were highest (fuel 1) and lowest (fuel 5) in aromatics as well as three other representative fuels of various compositions. Parametric studies were completed on fuels 1, 5, and 7 while more limited data was obtained on fuels 2 and 9. The run conditions and results of twenty-nine tests involving these five fuels are summarized in Tables IV and V.

Figures 20 and 21 show that the mean particle diameter of soot did not vary appreciably with aromatics or hydrogen content. Figure 22 shows a similar indifference to exhaust temperature. The relatively constant mean diameter of approximately 0.20 to 0.26 microns was in good agreement with data presented in references 4 and 10.

The trends for NO_x levels versus temperature are shown in Figure 23. The expected increase in NO_x with exhaust temperature is evident and the sensitivity was in reasonable agreement with the T63 engine test [Ref. 6] trends. However, the NO_x concentrations were approximately 100 times greater in the NAPC engine tests [Ref. 6]. Possible reasons for the different NO_x levels are the lower air temperature at the inlet of the NPS combustor and its effect on the "primary zone" and 2) different locations for the "exhaust temperature" measurement. Trends such as these which have been related to exhaust temperature could be similarly related to fuel/air ratio. Figure 24 reveals no correlation of aromatics content with NO_x levels.

TABLE III

Physical and Chemical Properties of Fuels (Ref. 6)

	1 (SUNTECH 1)	2 (SUNTECH 2)	3 (SUNTECH 3)	4 (SUNTECH 4)	5 Low Aromatic JP-5	6 Fuel Oil No. 2	7 Hydrocracked Gas Oil / JP-5	8 Diesel Fuel Marine / JP-5 50/50	9 High Aromatic JP-5	10 Oil Shale JP-5	Specif. MIL-T-5624L Require-ment
API Gravity @ 15°C	38.9	37.8	41.3	41.6	41.8	37.1	35.6	38.9	40.5	43.7	37.0-48.0
Distillation (ASTM) IBP °C	163	168	171	180	181	153	193	180	190	184	---
Recovered 10%, max.	190	227	192	202	199	218	204	204	204	193	205
Recovered 20%	207	242	203	210	203	232	209	213	208	196	---
Recovered 50%	247	257	227	228	217	266	226	237	218	205	---
Recovered 90%	276	272	261	264	243	317	272	297	246	231	---
End Point, °C, max.	297	281	276	282	261	333	288	323	264	257	290
Residue (ml), max.	2.0	1.8	1.4	1.4	1.2	2.8	3.6	2.9	1.4	1.2	1.5
Loss (ml), max.	0.9	0.2	0.1	0.5	0.2	0.0	0.4	0.0	0.5	0.4	1.5
Composition Aromatics (vol%),max.	28.5	19.8	22.8	18.6	15.9	25.0	26.4	18.6	22.7	21.8	25.0
Olefins (vol%), max.	1.79	0.81	0.75	0.79	0.79	1.40	0.86	0.70	1.62	1.60	5.0
Hydrogen Content,(wt%), min.	13.36	13.48	13.66	13.82	13.79	13.22	12.83	13.54	13.49	13.70	13.50
Smoke Point, mm, min.	17.0	18.0	20.0	21.0	21.0	17.0	14.0	16.0	21.0	21.0	19.0
Aniline - Gravity Prod., min.	5,360	5,557	5,811	6,140	--	5,661	4,254	5,648	5,471	6,022	4,500
Freeze Point, °C	-30	-24	-34	-34.5	-50.0	-3.0	-31.0	-10.5	-53.0	-49.5	-46
Viscosity @ 37.8 °C, (cSt)	1.78	2.27	1.62	1.74	1.58	2.60	1.77	2.06	1.50	1.38	---
Temperature @ 12 cSt, (°C)	-30.6	-20.6	-35.6	-31.7	-35.5	-13.3	-30.6	-23.3	-35	-34.4	---

TABLE IV

EXPERIMENTAL CONDITIONS FOR FUEL PROPERTY TEST SERIES

Fuel no.	Run no.	T_{air} (°R)	T_{ex} (°R)	P_c (psia)	$\dot{m}_{air}$ (lbm/sec)	f
1	1	464	1597	99	2.64	.0143
	2	488	1552	104	2.67	.0166
	3	486	1605	107	2.70	.0172
	4	492	1609	106	2.70	.0174
	5	498	1433	100	2.69	.0143
	6	495	1678	106	2.66	.0183
	7	494	1475	101	2.69	.0154
	8	501	1703	104	2.63	.0187
	9	483	1678	105	2.69	.0177
	10	485	1802	109	2.74	.0201
	11	487	1712	105	2.69	.0183
2	6	465	1610	101	2.71	.0140
5	1	492	1678	108	2.65	.0182
	2	492	1682	109	2.67	.0186
	3	499	1678	106	2.60	.0185
	4	497	1576	105	2.65	.0167
	5	497	1466	100	2.69	.0152
	6	497	1635	105	2.64	.0178
	7	497	1712	107	2.64	.0188
7	2	477	1660	100	2.62	.0145
	3	474	1450	---	2.60	.0146
	4	474	1515	106	2.61	.0157
	5	475	1678	109	2.57	.0180
	8	476	1690	113	2.74	.0179
	9	476	1754	112	2.67	.0187
	10	499	1470	101	2.64	.0146
	11	478	1538	106	2.71	.0159
	12	488	1534	107	2.68	.0161
9	1	464	1661	99	2.63	.0149

TABLE V

RESULTS FROM FUEL PROPERTY TEST SERIES

Fuel no./Run no.		T(.850)	T(.466)	T(.650)	d_{32} (μm)	NOx (ppm)	NO (ppm)
1	1	.390	.170	.290	.26	15	7
	2	.264	.160	.196	.30*	15.5	14
	3	.200	.137	.159	.37*	16.5	16
	4	.194	.137	.151	.36*	16	14.5
	5	.241	.200	.242	---	12	8
	6	.124	.091	.113	---	18	17.5
	7	.187	.140	.161	.36*	13	9.5
	8**	.134	.097	----	---	24	23
	11***	.315	.176	.232	.26	20.5	17.5
2	6	.470	.172	.293	.21	12	9
5	3	.175	.142	.196	---	24	22
	4	.335	.171	.247	.25	----	----
	5	.381	.214	.292	.25	12	9.5
	6	.259	.156	.214	.31*	21	18
	7	.284	.139	.205	.25	23	20.5
7	4	----	----	----	---	15.5	12.5
	5	.196	.069	.110	.24	22	19
	8	.201	.066	.120	.23	----	----
	9	.157	.064	.094	.26	----	----
	10	.297	.140	.207	.26	----	16
	11	.146	.103	.150	---	13	9.5
	12	.203	.112	.166	.31*	---	----
9	1	.430	.180	.320	.24	16	8

*questionable correlation (±.05 micron)
**Ferrocene additive @ 20 ml/gallon fuel
***12% Cerium Hex-Cem additive
@ 20 ml/gallon fuel

Figure 25 depicts a general decrease in visible transmittance with increasing temperature for fuels 1, 5 and 7. Similarly, Figure 26 shows a trend, for each individual fuel, of increasing mass concentration with increasing combustor exhaust temperature (or fuel/air ratio). The results of the T63 engine investigation by NAPC [Ref. 6] also revealed an increase in engine smoke number (which increases with particulate mass concentration) with increasing temperature. However, data from reference 10 indicated a cleaner burn in a combustor at higher temperatures. A possible explanation for this difference is that the T63 combustor utilized in this study has a small residence time and does not provide the time-at-temperature necessary for any appreciable soot consumption downstream of the primary combustion zone.

Fuel 1 (Figure 25) resulted in a significantly lower visible transmittance than fuel 5 (in agreement with reference 6), which indicated that fuels high in aromatic content had higher smoke numbers. For this reason, the decision was made to use fuel 1 to test the effectiveness of two smoke suppresant fuel additives. Test runs 8 and 11 utilized Ferrocene and 12% Cerium Hex-Cem respectively at concentrations of approximately 20 ml per gallon of fuel. Using equation 8 for the visible wavelength of .466 microns, Ferrocene and 12% Cerium Hex-cem resulted in approximately 10% and 35% reductions in soot concentration at the combustor exit.

It should be noted that the results from the initial investigation discussed above showed that the central zone near the combustor exit (where the transmission measurements were made) was of lower temperature than the outer annular region. This could present a region with large concentrations of soot, little effected by additives. The transmittance measurement was probably dominated by this low temperature, central core region.

In an earlier study [Ref. 4] the above additives resulted in significantly greater reductions in soot concentration. However, that investigation used a combustor with a significantly larger residence time than the T63 combustor. There was some concern that the reduced effectiveness of the additives was due to the unheated combustor inlet air. This prompted a request by NPS for tests at NAPC using 12% Cerium Hex-Cem in the T63 engine (vs. the T63 combustor at NPS). NAPC conducted these tests and observed a 70% reduction in SAE smoke number (SN) (Ref. 11). SAE SN can be converted to soot concentration (with questionable accuracy) per reference 12. Transmittance was also a strong function of temperature for fuel number 1 (Fig. 25). The transmittance with no additive from run number 6 (Table V) was "corrected" to .069 at an effective temperature of 1712 °R (Table IV). The results are shown in Table VI.

TABLE VI

SUMMARY OF TEST RESULTS WITH 12% CERIUM HEX-CEM

	$\dot{M}_{air}$ (lb^m sec)	f	Combustor inlet air temperature (°R)	Additive (wt. %)	T_{ex} (°R)	% reduction in soot concentration
NPS T63 combustor	2.69	.018	495	.63	1710	35 (combustor exit)
NAPC T63 engine	3.17	.019	860 (approx.)	.77	1840	95 (engine exit)

The significant reduction in additive effectiveness in the NPS combustor is presently thought to result from (1) the lower inlet air temperature (and, consequently lower exhaust temperature) and/or (2) the

location of the transmittance measurement in the NPS combustor as discussed above. Earlier tests (Ref. 3 & 4) have indicated that the additives are not as effective when exhaust temperatures are less than 1800°R.

3. Centerline Temperature Profiles

The stagnation temperature probe used in the initial tests was designed to minimize radiation effects by positioning the thermocouple within a recessed area which was vented radially. The probe failed during an early test due to lack of adequate cooling water flow. After some modifications, testing was resumed. The new probe (see Fig. 27) had a thermocouple which extended out the tip of the water jacket. The tip was encased in Omega High Temperature Thermocouple Cement to the point where the thermocouple was imbedded just beneath the surface of the cement. This design is not ideal but was considered adequate for measuring approximate stagnation temperatures in this initial study. No corrections were made for radiation effects.

Two fuels (numbers 1 and 5) were tested at two fuel-air ratios (.019 and .021). A summary of test conditions is presented in Table VII. Fig. 28 presents the measured temperature profiles along the combustor centerline.

TABLE VII

EXPERIMENTAL CONDITIONS FOR TEMPERATURE PROFILE MEASUREMENTS

run number.....	1-1	1-2	5-1	5-2
fuel number.....	1	1	5	5
T_{air} (°R).....	501	500	504	508
$\dot{M}_{air}$.....	2.60	2.59	2.58	2.54
f.....	0.019	0.021	0.019	0.021
P_c (psia).....	120	115	106	107
T_{ex} (°F).....	1247	1403	1235	1372

As expected, both fuels showed almost uniformly higher temperature profiles at the higher fuel-air ratios, but the peak temperature points also moved aft. For fuel 1 the peak temperature point moved from about 4.7 inches to about 5.0 inches from the fuel nozzle. For fuel 5 the peak temperature point moved from about 5.0 inches to about 5.3 inches from the nozzle. In both cases the movement was about 0.3 inches.

The aft movement of the peak temperatures apparently results from the changing fuel distribution and velocity at the higher fuel flow rates. Although the temperature measurements were only qualitative, several important characteristics were apparent. The primary combustion region along the centerline ended at approximately 5 to 5 1/2 inches from the fuel nozzle. The low temperatures also could indicate that the majority of the heat release occurs in an annular area (although the thermocouple may have been inaccurate as discussed above). These results indicate that the soot concentration (and possibly size) may vary significantly across the combustor at any particular axial position. It is also interesting to note that the fuel with higher aromatic content (fuel 1) had higher centerline temperatures and combustion pressures.

4. Particulate Collection

The original particulate collection apparatus discussed above was slightly modified for this series of tests. Since the combustion chamber was pressurized to approximately six atmospheres, the vacuum pump which was installed to enhance probe flow rate was not needed. In order to maintain isokinetic conditions, the flow in the sampling line actually had to be slowed by partially closing the control valve with the vacuum pump removed. Near the fuel nozzle the valve had to be almost completely closed, and the probe flow rate was negligible.

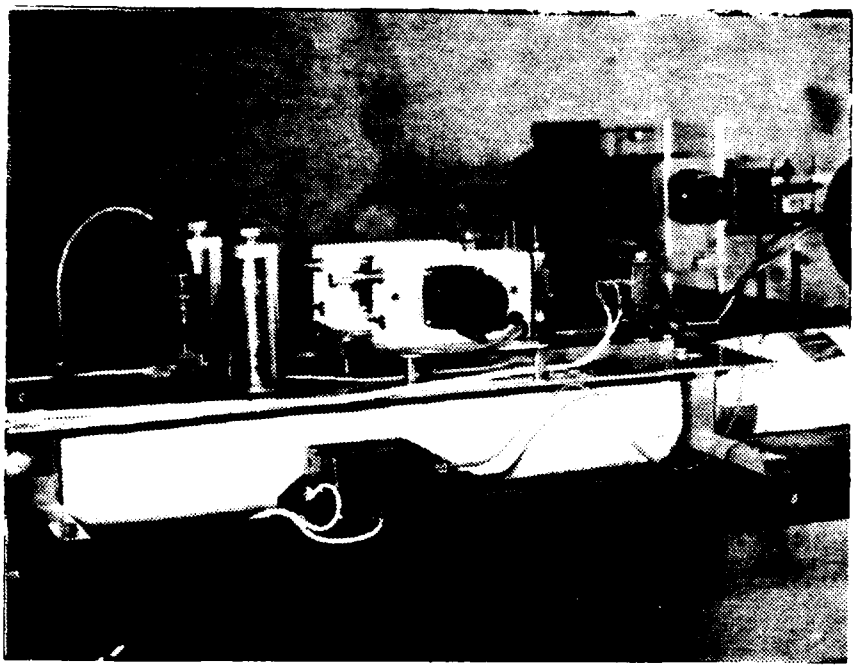

Figure 6. Turbine Flowmeter and Additive Metering Pumps

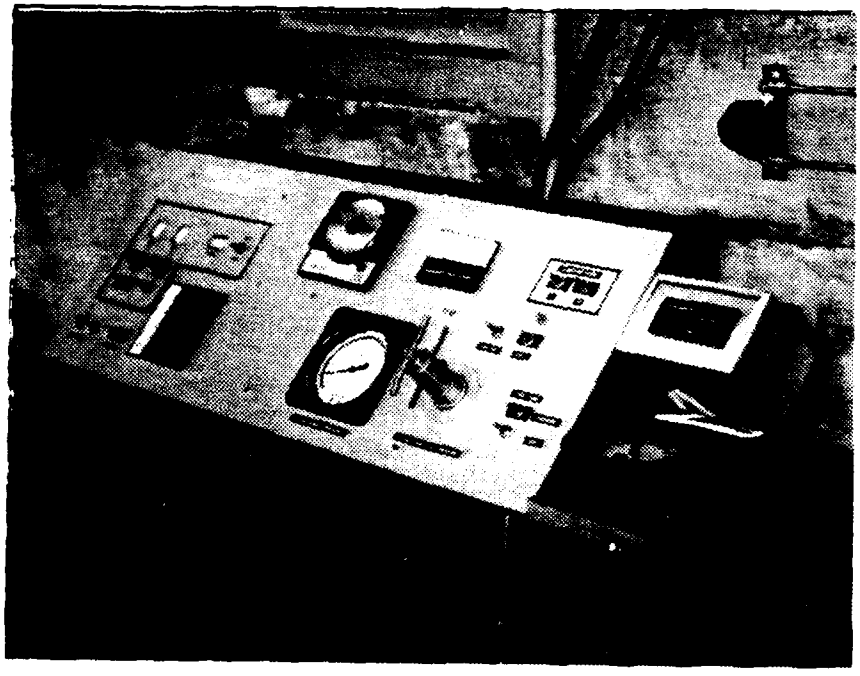

Figure 5. T63 Control Panel.

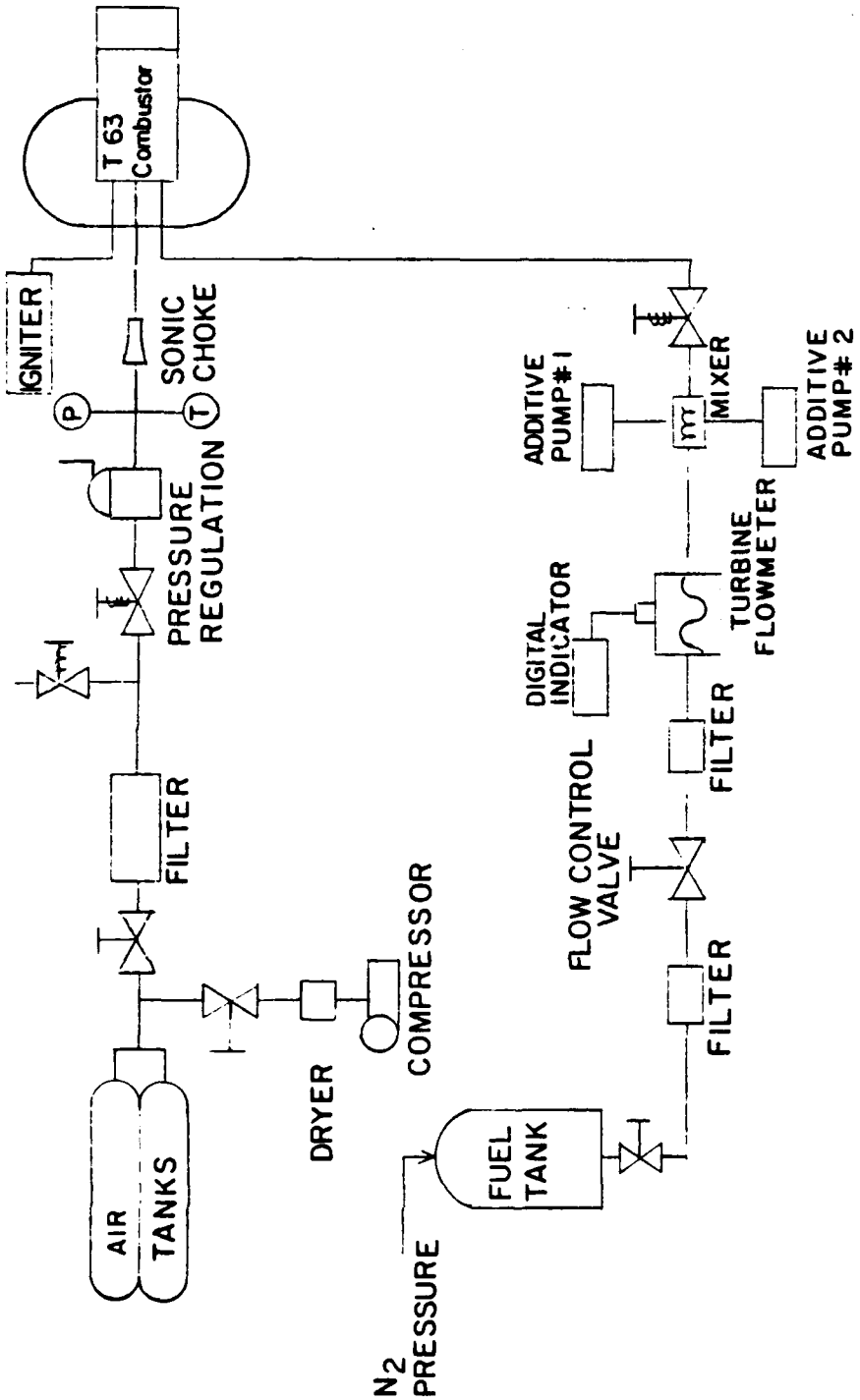

Figure 4. Schematic of T63 Test Cell Facility

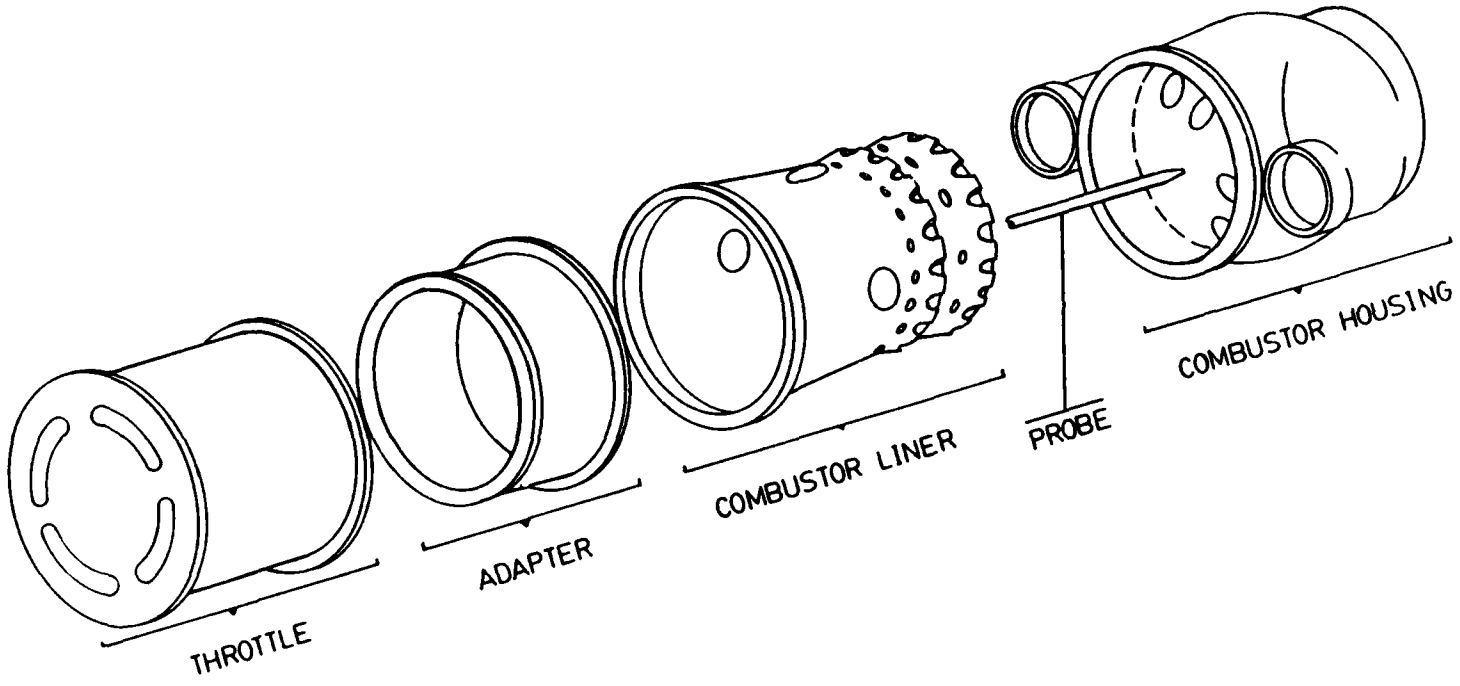

Figure 3. Schematic of Combustor Components

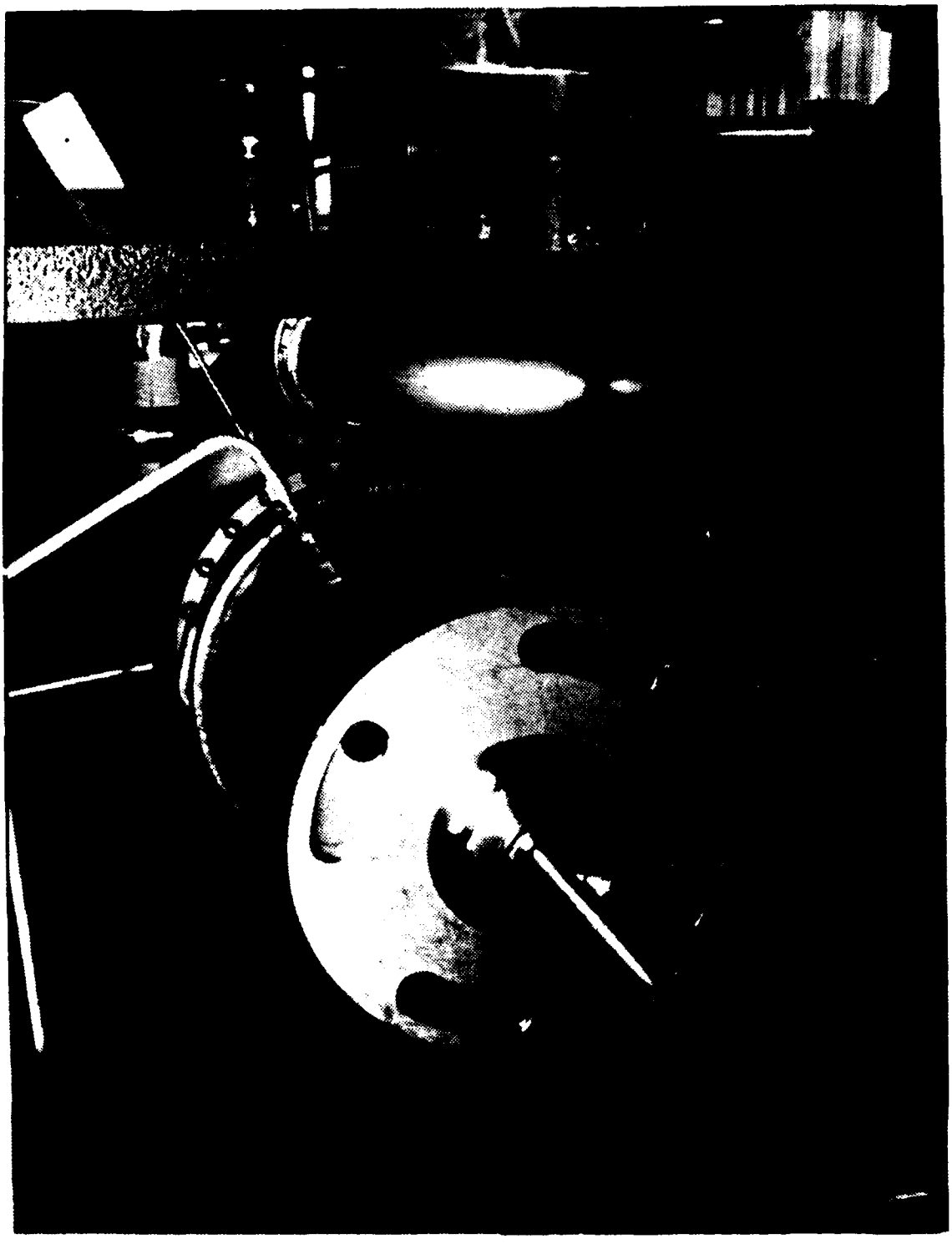

Figure 2. Combustor, Aft View.

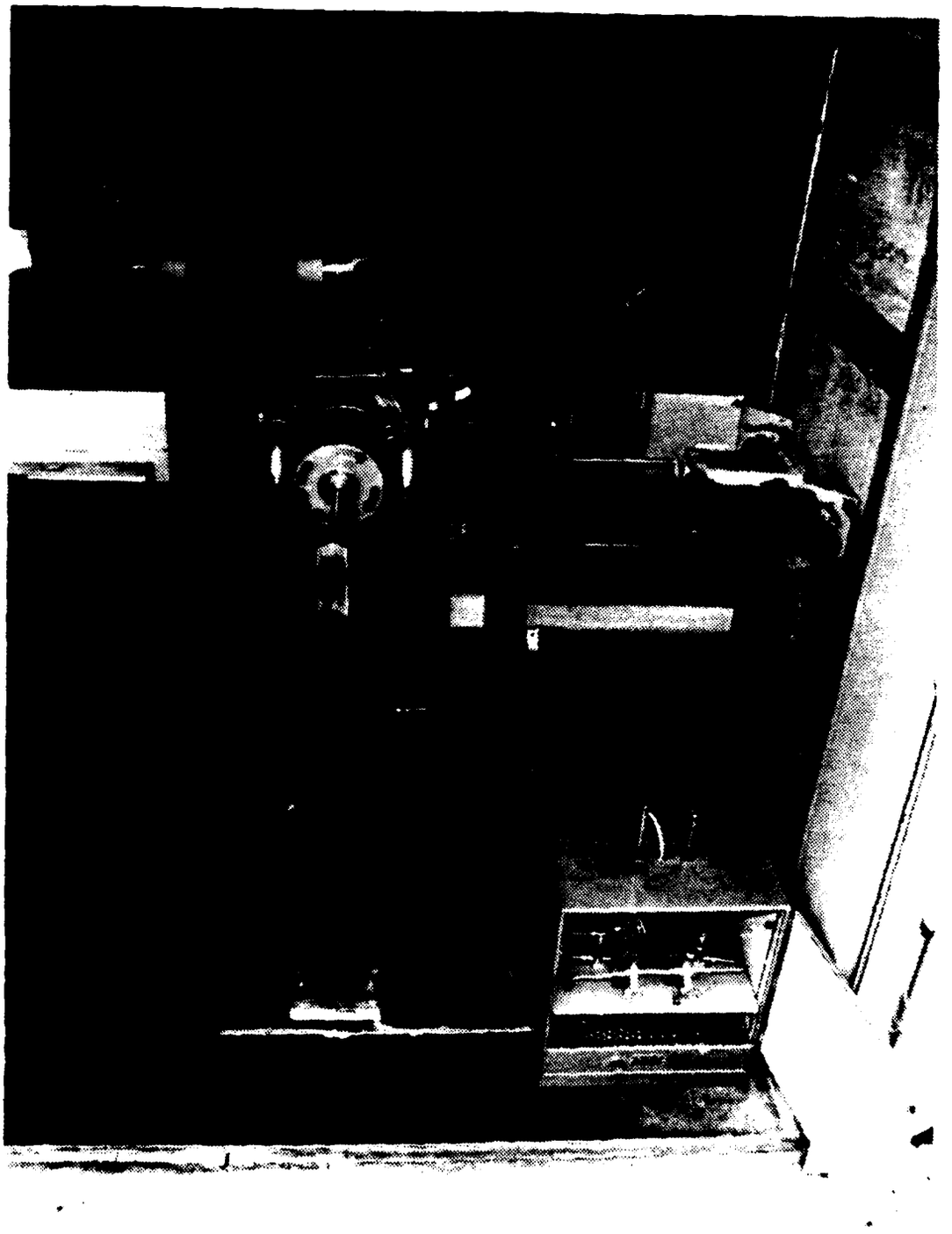

Figure 1. Combustor Test Cell

transmittance) with higher exhaust temperature was the result of a greater production of soot within the combustor while a short residence time in the T63 inhibited the usual subsequent consumption of the soot which has been formed.

12% Cerium Hex-Cem was found more effective in reducing soot concentration than Ferrocene. However, the test conditions and measurement locations were not optimal for evaluating additive performance. The limited data were in agreement with results from other studies (Ref. 4), showing no effect of the additives on D_{32} of the soot particles.

and the use of slower cooling rates (hotter cooling water) should also be investigated to determine if they have any effect on the collected sample.

The decreased effectiveness of smoke-suppressant fuel additives in the present combustor in comparison with T63 engine test data was apparently due in part to the low air inlet temperatures. A (hydrogen fuel) vitiated air heater is, therefore, being added to the present air supply system to permit the effects of inlet air temperature to be investigated.

2. Fuel Composition and Additive Effects

Repeated tests with several fuels indicated reasonable and well-correlated soot particle diameters from 0.21 to 0.26 microns. NOx concentrations were temperature dependent with values ranging from 12 to 24 ppm. A refractive index for soot of 1.95 - .66i with $\sigma = 1.5$ was found to most consistently correlate the transmission ratios using all three wavelengths.

Parametric studies were made on three of the five fuels tested. In all respects the different fuels manifested the same trends. Fuels 1, 5, and 7 exhibited 1) increasing NOx levels with increasing combustor exhaust temperature or fuel/air ratio; 2) decreasing transmittance with increasing combustor exhaust temperature or fuel/air ratio; 3) increasing mass concentration with increasing combustor exhaust temperature or fuel/air ratio; and 4) constant particulate size with changing fuel composition and exhaust temperature. The decreasing transmittance was a function of the increasing mass concentration since particulate size was found not to vary as a function of temperature.

The results for particle size, NOx concentration, and mass concentration were in qualitative agreement with the results presented in reference 6. It is felt that the apparent increase in mass concentration (decreasing

The present light transmission path has been found to pass through a highly non-uniform combustion zone. Low temperatures and high soot concentrations apparently exist in a large central recirculation zone surrounded by an annular region of higher temperature and lower soot concentrations. Measurements are needed within the annular region since it more nearly represents the exhaust characteristics. In addition, the smoke suppressant additives are probably more effective within this higher temperature region.

An additional light transmission path is currently being added to the T63 combustor within the aft annular exhaust region. In addition, two ports are being added at each location for measurements of scattered laser light at two forward angles.

The NO_x sampling apparatus appeared to work adequately except for occasional fouling of the sampling line with soot and/or liquid fuel. These problems generally occurred during the combustor ignition phase at high fuel-air ratios.

The thermocouple probe can be used to obtain good qualitative temperature profiles along the combustor centerline. The probe needs to be modified to shield the thermocouple from radiation and to permit direct exposure to the gases. Other thermocouples are needed to better define the thermal environment and how it is affected by operating conditions, fuel composition and additives. Five radially positioned thermocouples are currently being added to the T63 combustor for this purpose.

The puff-like structures observed in the SEM photographs of the collected samples appear to be a by-product of the sampling technique. To obtain more representative samples for determination of soot size, sampling times should be greatly reduced, perhaps to approximately one second. Nitrogen dilution

V. CONCLUSIONS AND RECOMMENDATIONS

1. Experimental Apparatus

The mean soot size (D_{32}) data obtained using the three-wavelength transmission measurements appears to be in reasonably good agreement with the SEM photographs of collected soot. However, the optically measured D_{32} of 0.21 to 0.26 microns is larger than the dominant individual particle size (0.07 - 0.12 microns) observed in the photomicrographs. A few larger particles present in a large number of small particles results in D_{32} being closer to the larger diameter. It is not known whether the few larger particles actually exist within the combustor (as the optical method implies) or are a result of the sampling system. An earlier study (Ref. 4) used an extraction probe in the exhaust duct of the motor. Soot agglomerates were observed with diameters between 0.05 and 0.30 microns.

Several improvements can be made to enhance the quality of the data obtained from the light transmission apparatus. The present method used a "light-source-off" technique to minimize the effects of combustion generated light at the measured wavelengths. A better method is to use a light-chopper between the light source and combustor. A phase-lock amplifier then passes only photodiode output in phase with the chopped light source. Measurements of the ratio of light intensities at two large scattering angles can also result in determination of D_{32}, without having to know the refractive index of the soot. However, these measurements generally are limited (for single scattering) to regions where the transmittance is greater than approximately 80%.

Figs. 37 and 38 suggested a possible way of eliminating the puff-like structures if only particle size data are desired. The 8.0 micron membrane from run D did not exhibit any of the 25 micron, puff-like structures. Although run D lasted for 30 seconds, it had a very low flow rate. The number of particles which entered the probe had to have been much lower than in other runs. Thus, the puff-like structures could possibly be eliminated by even shorter sampling times.

D. SUMMARY OF CURRENT APPARATUS MODIFICATION

Some of the required modifications to improve the quality of the obtainable data have been discussed above. Modifications currently being made to the apparatus are listed below:

1. Addition of a (hydrogen fuel) vitiated air heater to provide more realistic air inlet temperatures. This will allow the effects of air inlet temperature on the effectiveness of the smoke-suppressant fuel additives to be investigated.
2. Addition of a light chopper and phase-lock amplifier in the light transmission measurement apparatus to eliminate combustor generated light at the monitored wavelengths.
3. Addition of a second set of access ports to permit optical measurements in the combustor exhaust duct.
4. Addition of ports to permit determination of soot size by using measurements of scattered laser light at two forward angles.
5. Addition of five radially positioned thermocouples to improve the temperature mapping within the combustor.

diameter, independent of distance from the fuel nozzle. Some almost spherical agglomerates were also present with diameters between 0.2 and 0.3 microns. It is not known how much of the agglomeration process occurs in the combustor vs. in the sampling system. However, the light transmission experiments measured mean (D_{32}) soot sizes between 0.2 and 0.3 microns. The optical method is inherently biased to the larger diameters.

The large, 25 micron, spheres seemed to be associated with the extractive probe sampling technique. Similar structures were observed by Samuelson [Ref. 9]. He had obtained these puff-like structures when using high overall sample transport temperatures and lower cooling rates. A "plate-like" structure had been observed when using higher cooling rates. Samuelson concluded that the plate-like structure had been caused by water condensation in the sample; the puff-like structures showed only slight evidence of any moisture. Based on these results, water condensation was not considered to be a problem in the present investigation, even though nitrogen dilution was not used and the probe cooling water was at 70°F.

Samuelson [Ref. 9] also suggested a scenario for the formation of the puff-like structures. A mixture of soot particles and fuel (undergoing pyrolysis) entered the probe. In the probe the mixture was slowly cooled, which promoted the formation of long chains of aggregated spheroids. Some of these chains deposited across the pores of the filters. The chains built up and eventually clogged the pore. This scenario was used to explain the existence of puffs of roughly the same size as the filter pores. It may also explain the results obtained in the present investigation, (where high sampling rates are used), even though the puffs were now three to four times bigger than the filter pores.

approximately 30 seconds to minimize the soot collected (based on results of the initial test series discussed above). The purpose of these tests was to obtain particle data, not soot concentration levels. Run E was made with a longer collection time in an initial attempt to obtain concentration data. This run resulted in large amounts of soot, which precluded the use of the scanning electron microscope for measuring particle size. The filter membranes were weighed before and after each run in order to determine the weight of the sample collected. However, the membranes employed for concentration measurements should be fiberglas instead of the Nuclepore membranes which were used in these tests. In run E a 2.5 mg. sample was collected in 180 seconds. This weight was divided by the collection time and the sample flow rate to yield a soot concentration of approximately 0.24 mg/liter.

The tests which used short sampling times (A through D) were made to obtain soot size characteristics between the fuel nozzle and the location of the peak centerline temperature. Figures 29 through 38 are SEM photographs of the filters. It was apparent from the filter coloration that the soot concentration increased (as expected) with distance from the fuel nozzle.

In Samples A, B and C large "puff" like shapes can be seen on the 8.0 micron membranes (Fig. 37). These results were similar to the earlier data (Fig. 15) collected at the aft end of the combustor. Sample D was the only one that lacked any of these structures (Fig. 38). These structures were either spherical or appeared as several spheres combined in chains. The individual spheres were about 25 microns in diameter. Under high magnifications (Fig. 29, 31, and 33) these larger spherical shapes were seen to consist of individual and agglomerations of small spherical particles. The small individual spherical particles were approximately .05 to 0.1 microns in

There are other errors inherent in the use of an extractive probe. These errors include (1) composition changes due to catalytic reactions within the probe (although stainless steel is one of the least reactive tube materials other than quartz [Ref. 13]), and (2) the time-averaging characteristic of a sampling probe when used in a turbulent flame. Also, the very presence of the probe creates a fluid dynamic and/or thermal diturbance to the flow.

A summary of the test conditions for the particulate sampling runs is presented in Table VIII. Runs A through D used a short sampling time of

TABLE VIII

EXPERIMENTAL CONDITIONS FOR PARTICULATE SAMPLING TESTS

Run.....	A	B	C	D	E
Fuel number.....	5	5	5	5	5
T_{air} (°R).....	501	508	526	522	508
$\dot{M}_{air}$ (lbm/sec).....	2.17	2.15	2.11	2.11	2.20
f.....	0.020	0.020	0.021	0.020	0.020
P_c (psia).....	99	99	98	98	101
T_{ex} (°F)	1275	1299	1286	1269	1308
Weight Change for:					
0.2 micron filter (mg)...					+0.4
8.0 micron filter (mg)...					+2.1
total (mg).....					+2.5
Sampling Time (sec).....	30.0	30.4	30.5	30.7	180
Sampling Position, (aft of fuel nozzle, inches).....	4.38	3.38	2.38	1.38	4.38
Sample Flow Rate (cc/sec)..					57.7
Oven Temp. (°F).....	171	171	173	173	171
Hose Temp. (°F).....	180	180	179	181	180

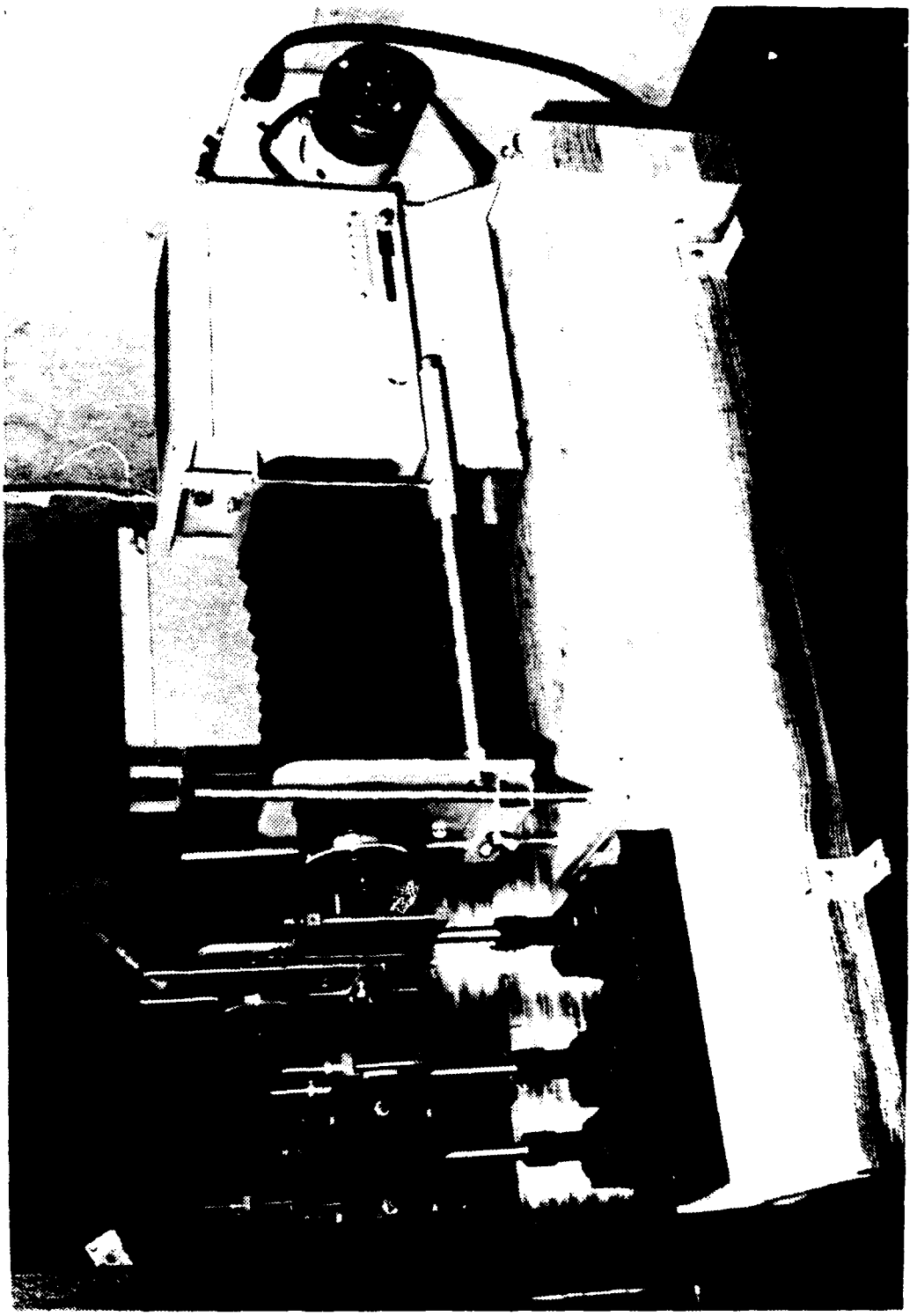

Figure 7. Collimated White-Light Source

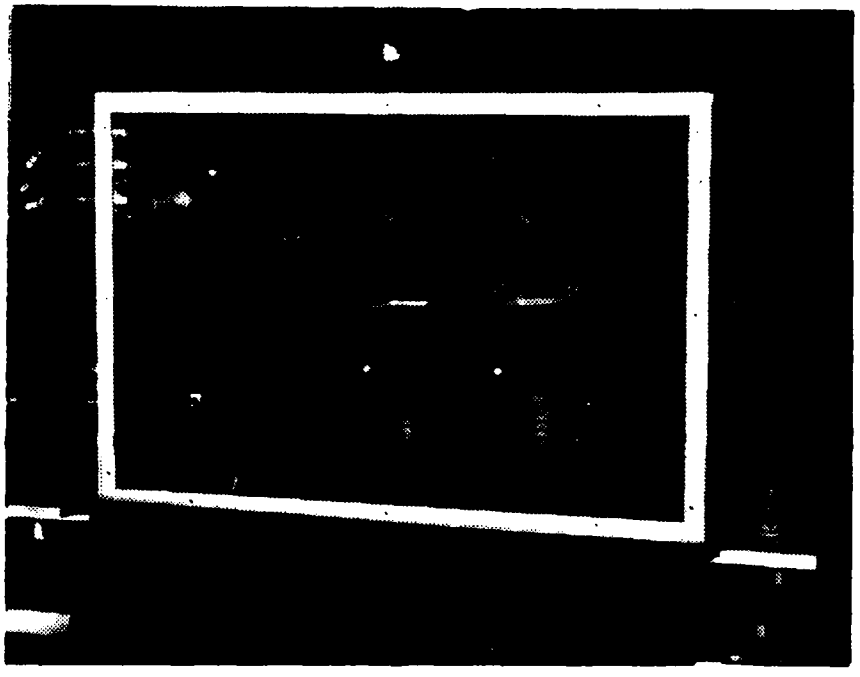

Figure 8. Three Wavelength Optical Detector.

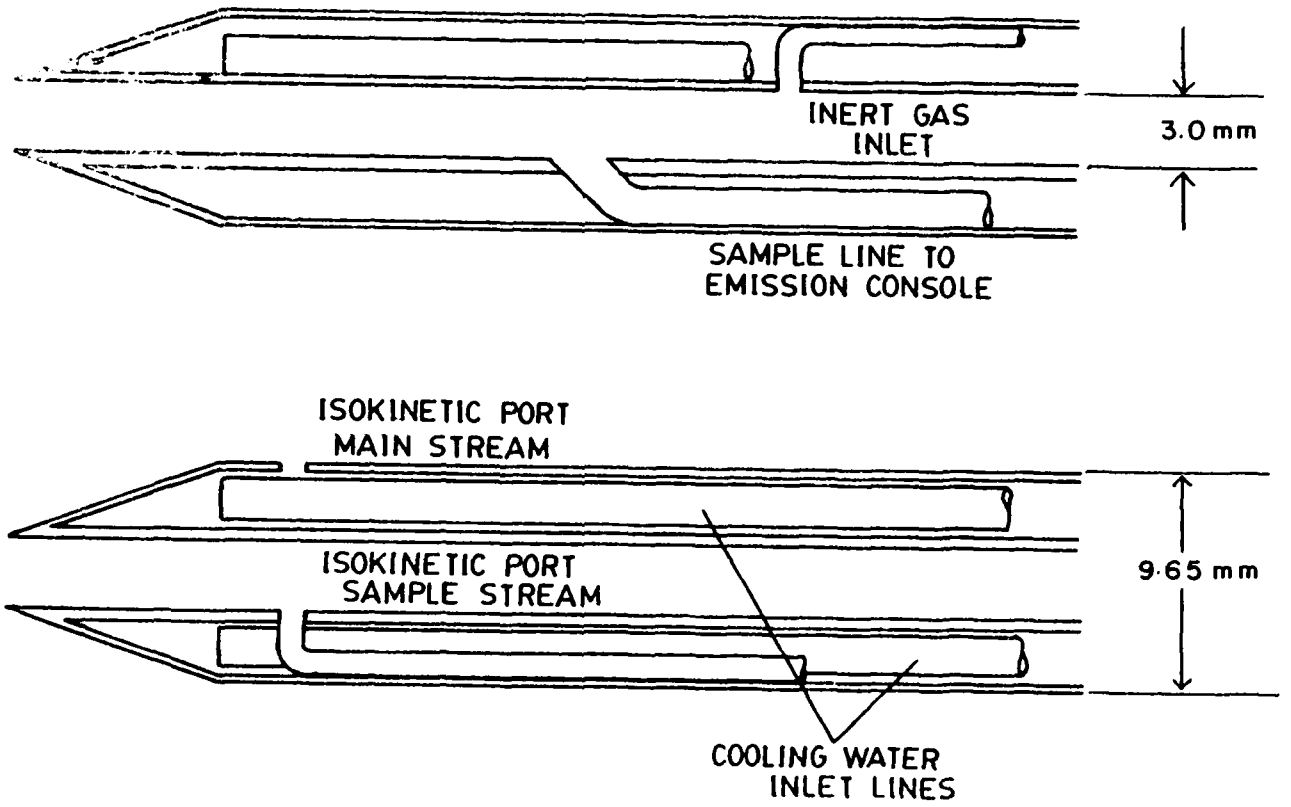

Figure 9. Schematic of Water Cooled Sampling Probe

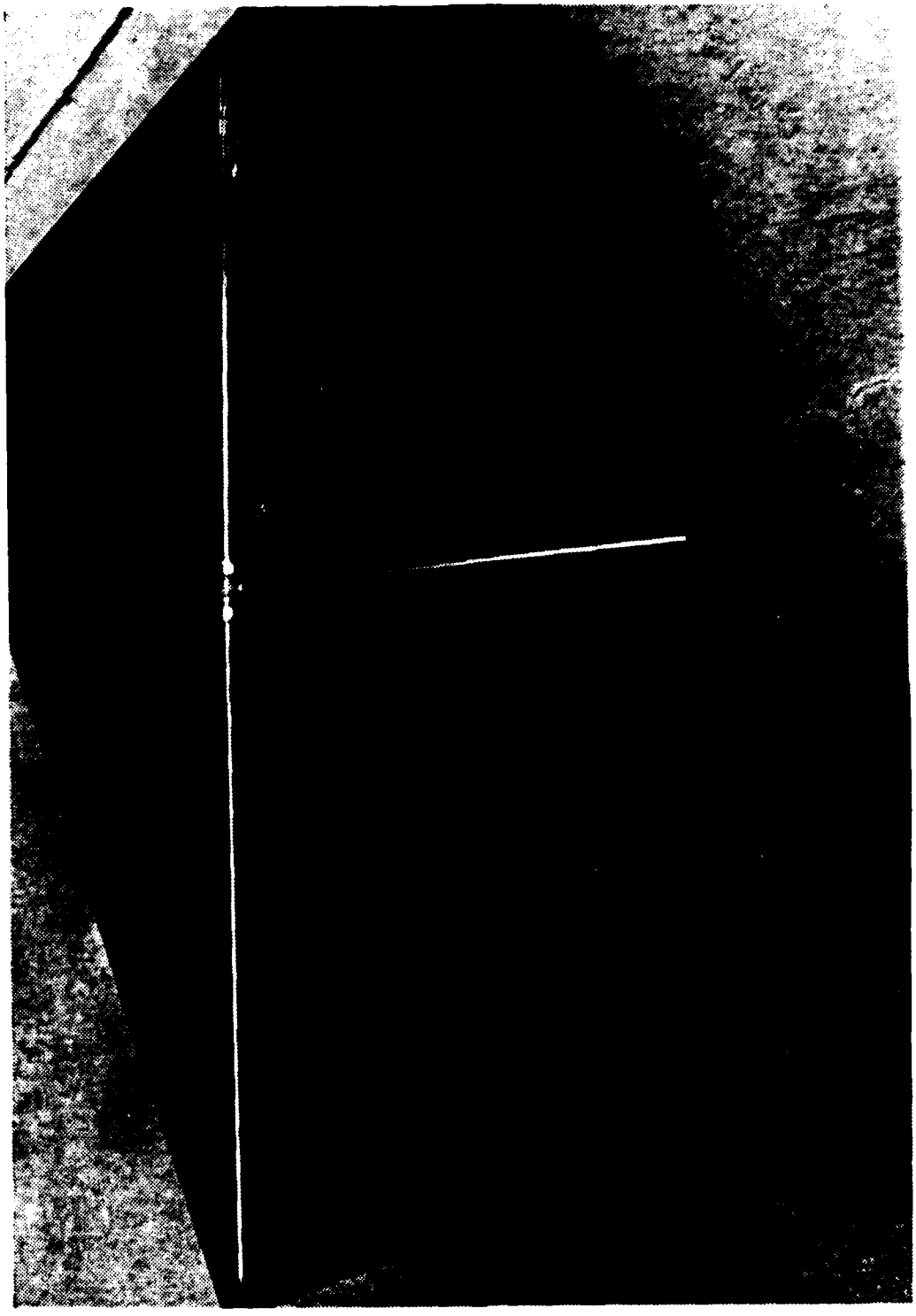

Figure 10. Sampling Probe

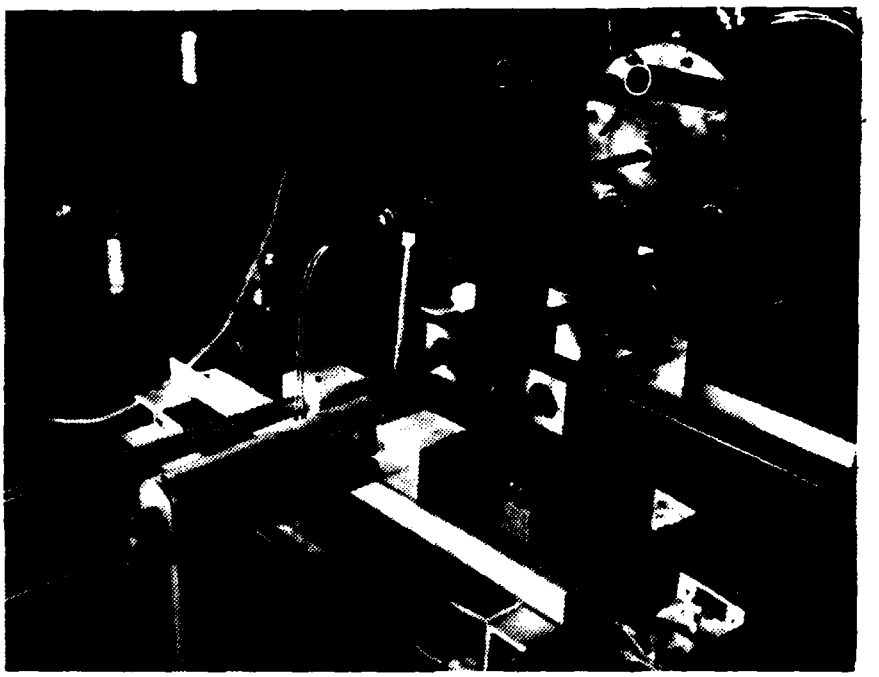

Figure 11. Exhaust Chamber, Temperature Probe and Holder.

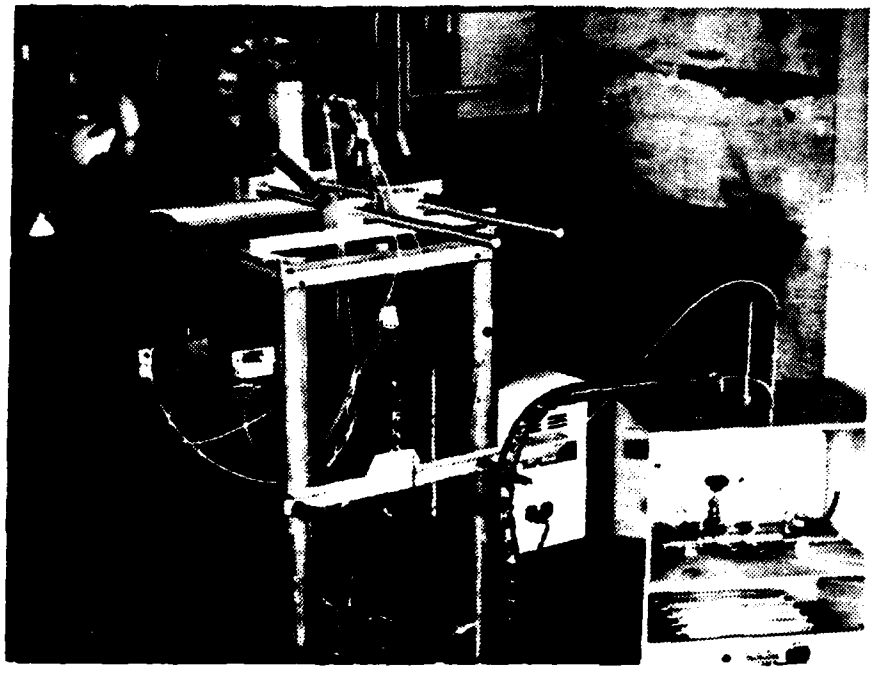

Figure 12. T63 Combustor with Sampling Apparatus.

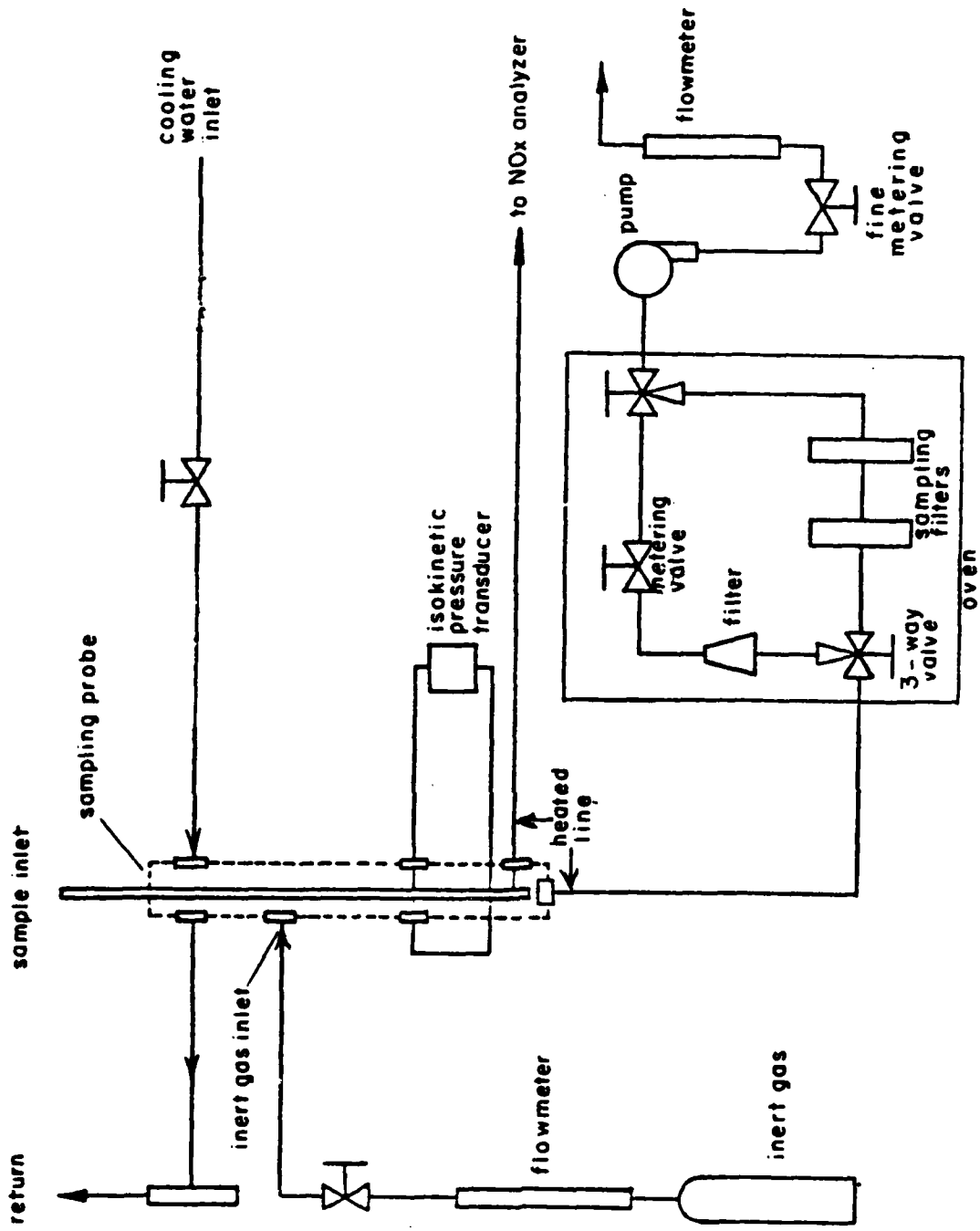

Figure 13. Schematic of Sampling Probe Apparatus (adapted from Ref. 9)

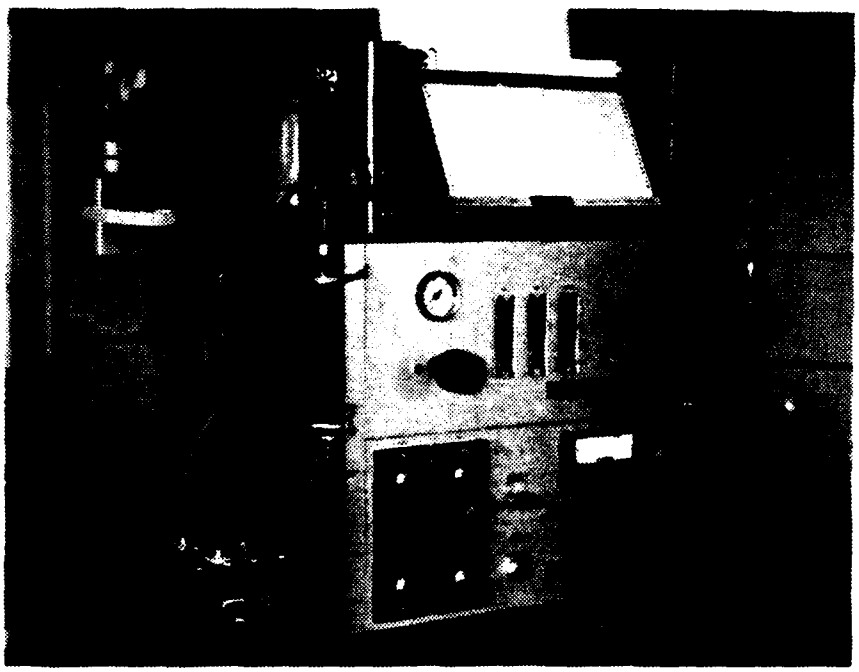

Figure 14. **Nitrogen Oxides Analyzer.**

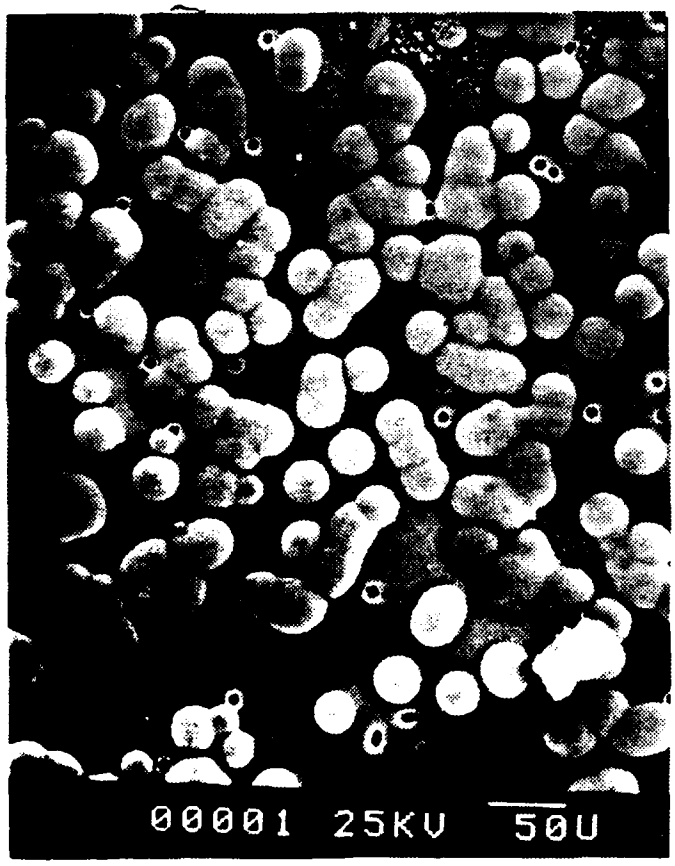

Figure 15. SEM Photograph, 8μm Filter, Gold Plated

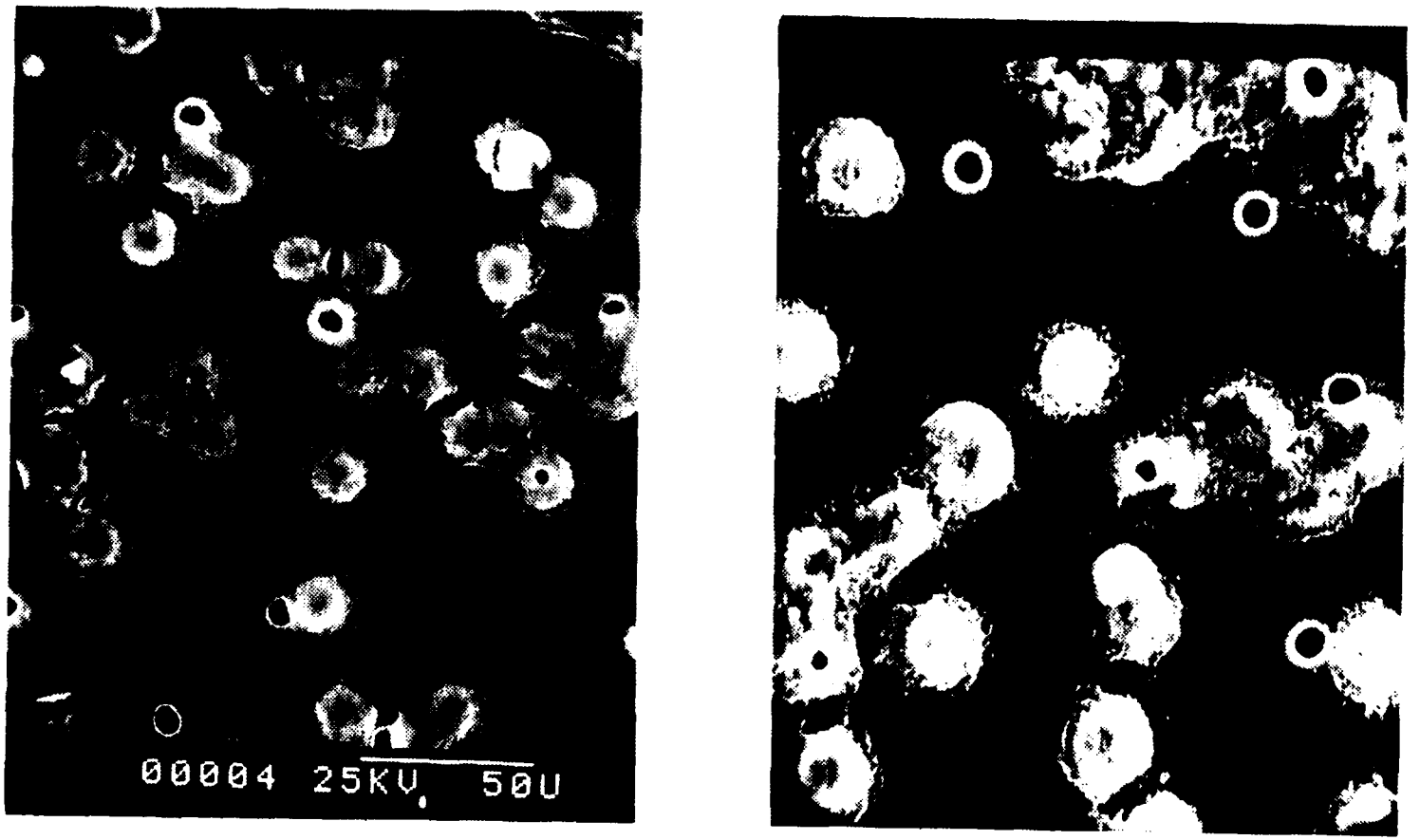

(a) (b)

Figure 16. SEM Photographs, 8μm Filter, Aluminum Plated; (a) Hitachi S540 (b) Cambridge S4-10 (500X)

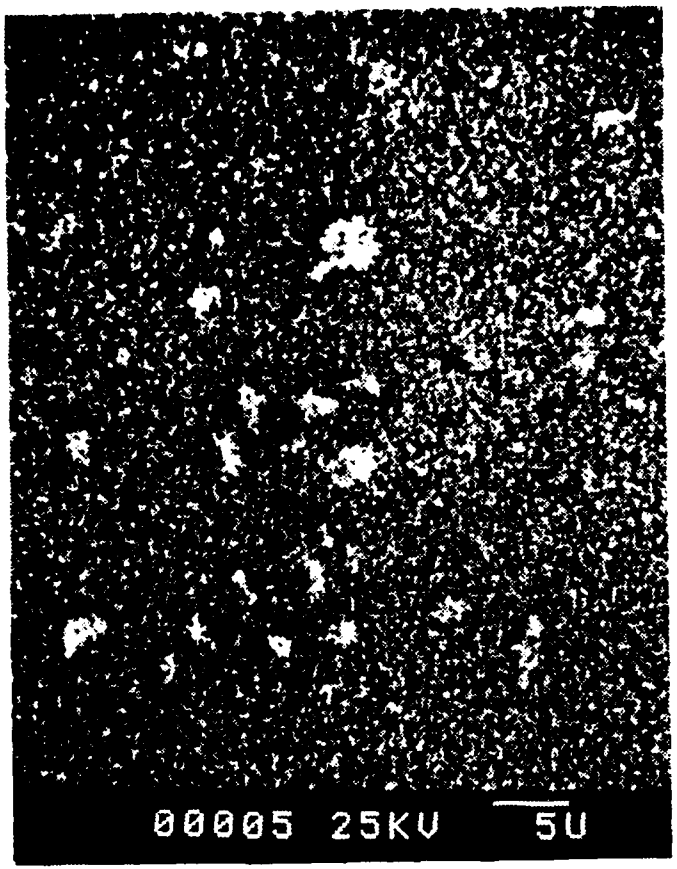

(a)

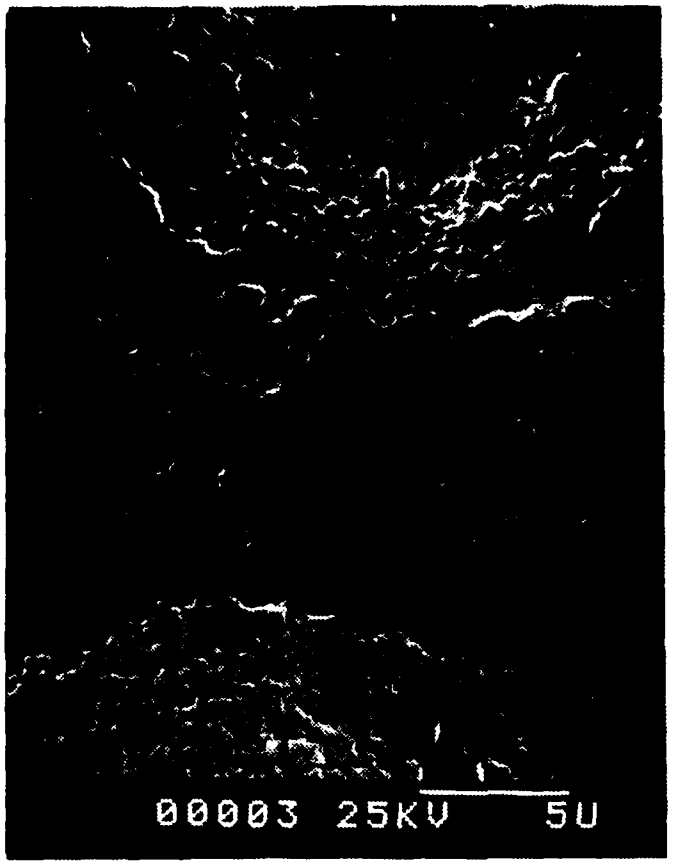

(b)

Figure 17. SEM Photographs, 8μm Filter, Hitachi S540: (a) Gold Plated, (b) Aluminum Plated

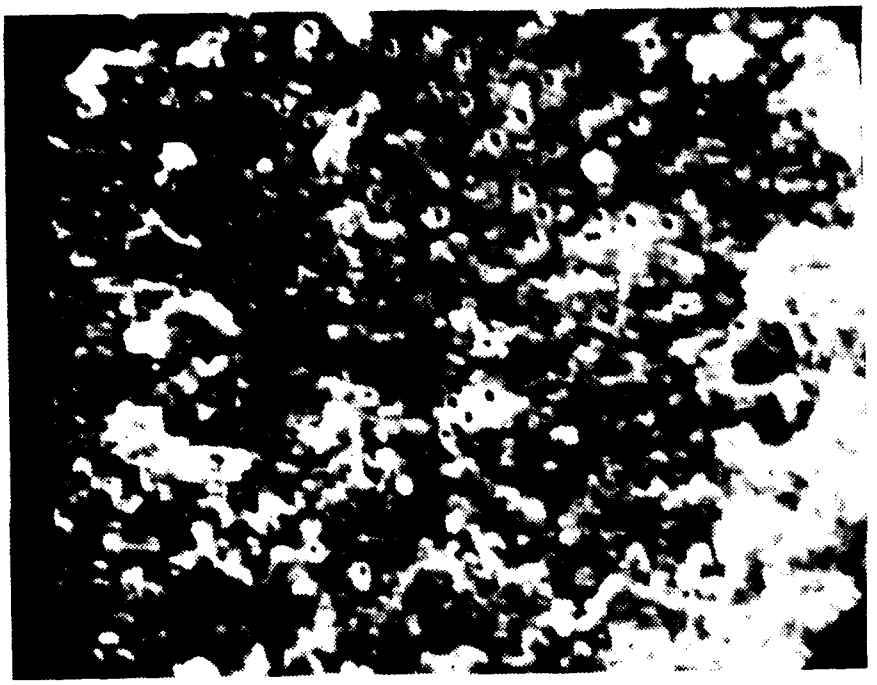

Figure 18. SEM Photograph, 0.2μm Filter, Cambridge S4-10 (10,000X), Aluminum Plated

(a)

(b)

Figure 19. SEM Photographs, .2μm Filter, Aluminum Plated

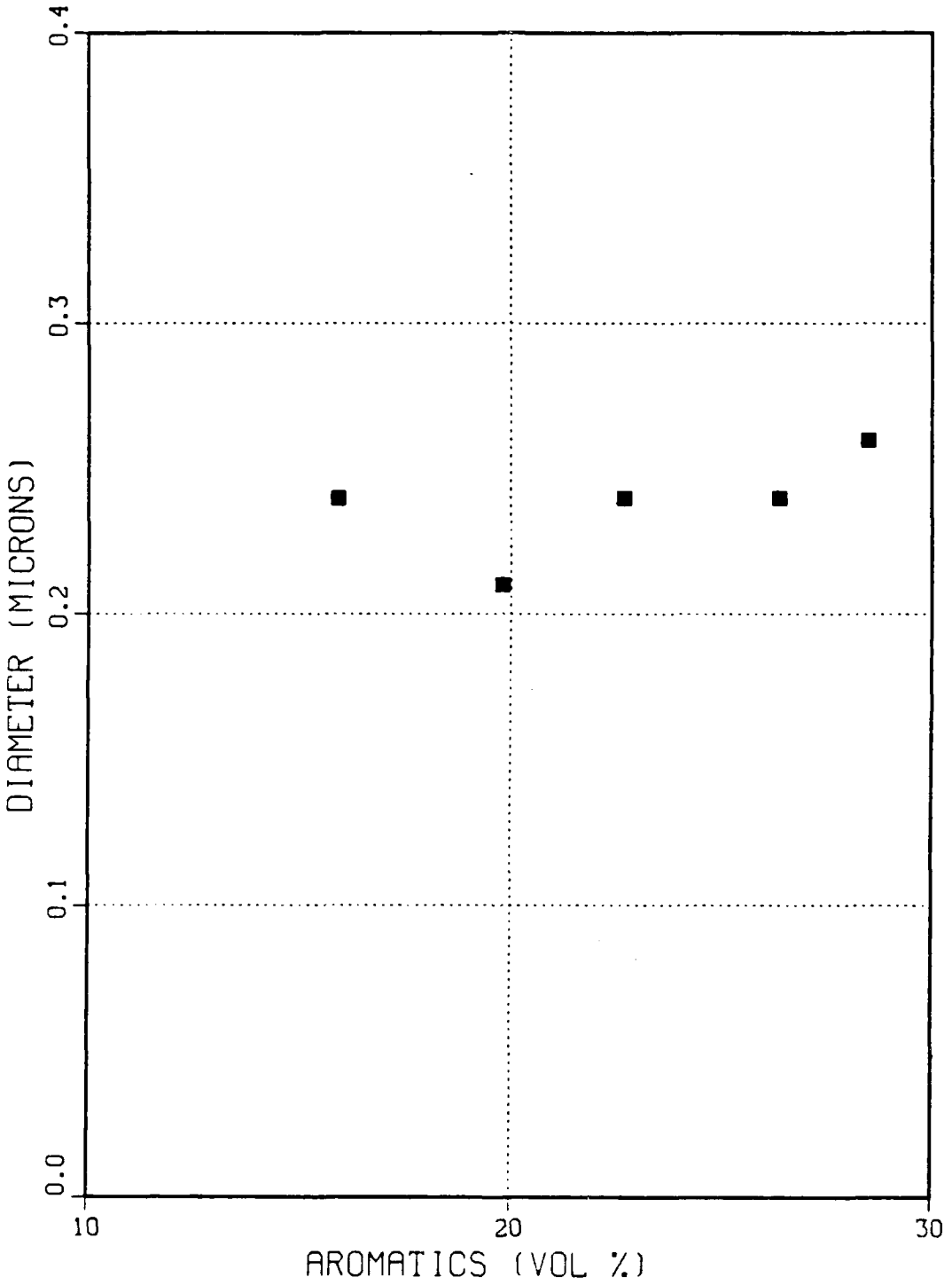

Figure 20. Particle Size vs. Aromatics Content

Figure 34. SEM Photograph, 0.2µm Filter, Run C

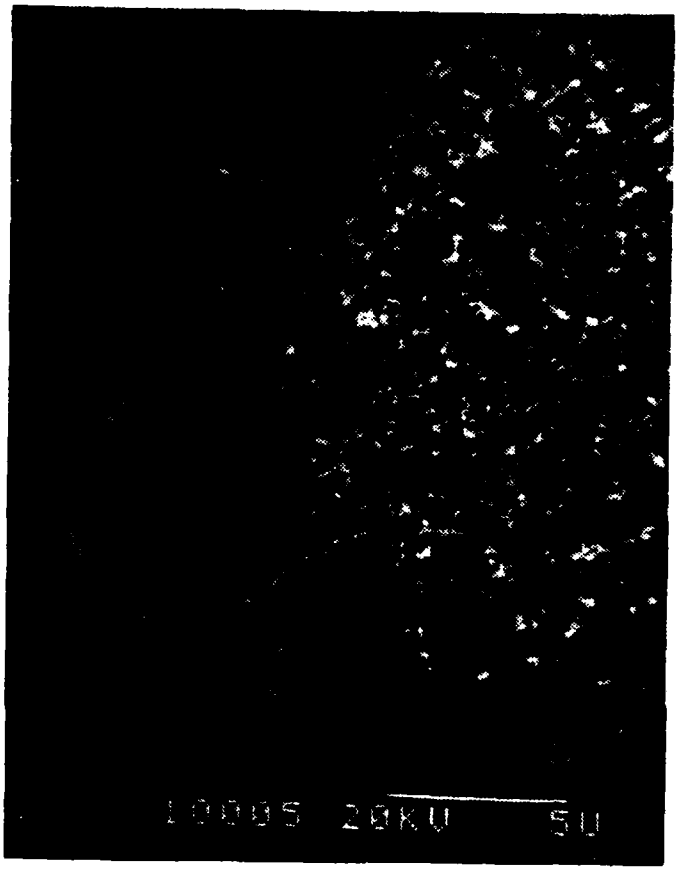

Figure 33. SEM Photograph, 8.0μm Filter, Run C

Figure 32. SEM Photograph, 0.2μm Filter, Run B

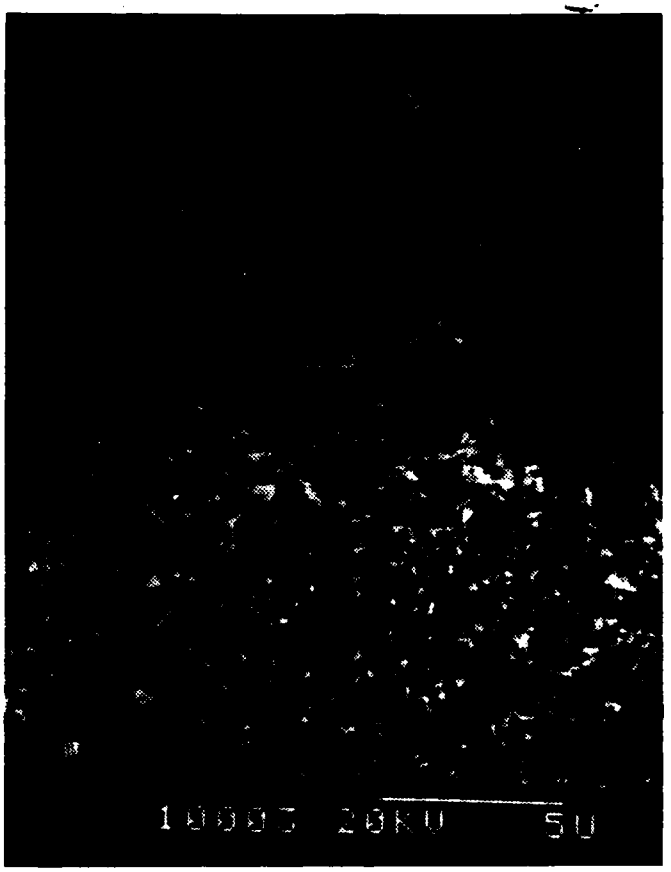

Figure 31. SEM Photograph, 8.0μm Filter, Run B

Figure 30. SEM Photograph, 0.2μm Filter, Run A

Figure 29. SEM Photograph, 8.0μm Filter, Run A

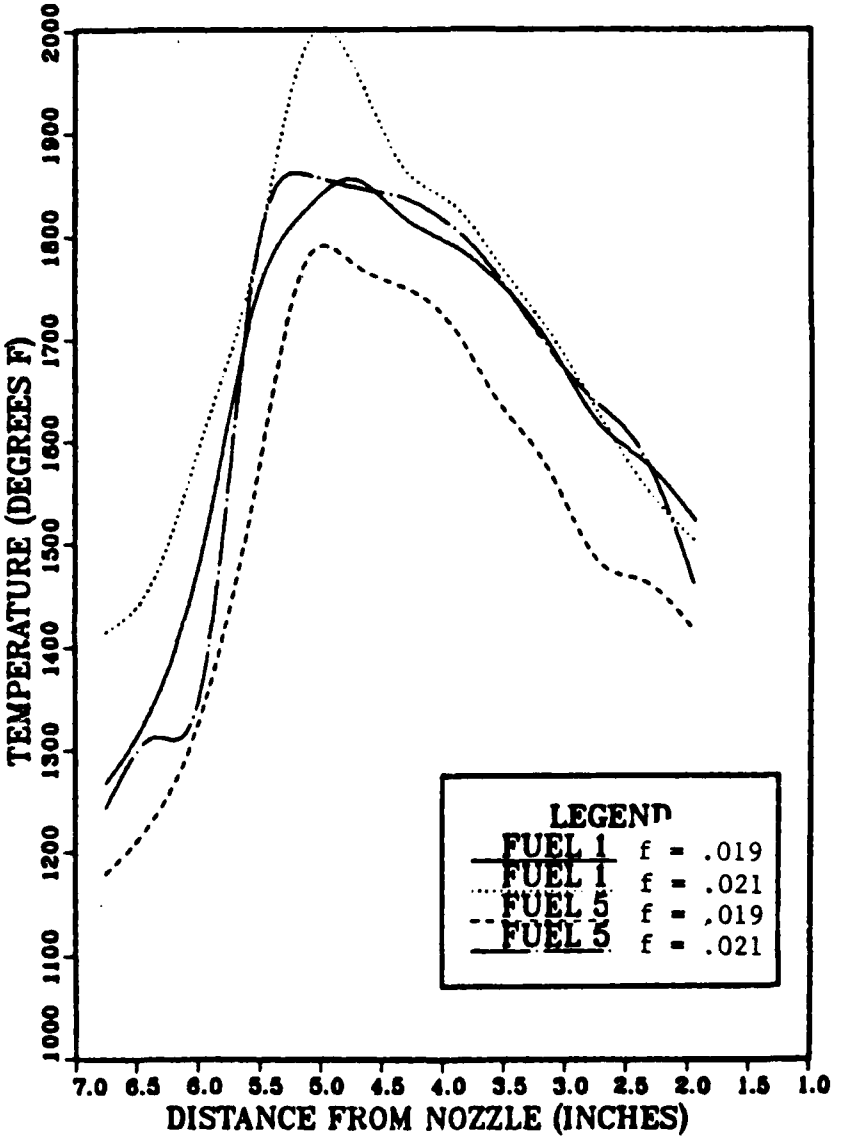

Figure 28. Axial Temperature Profiles

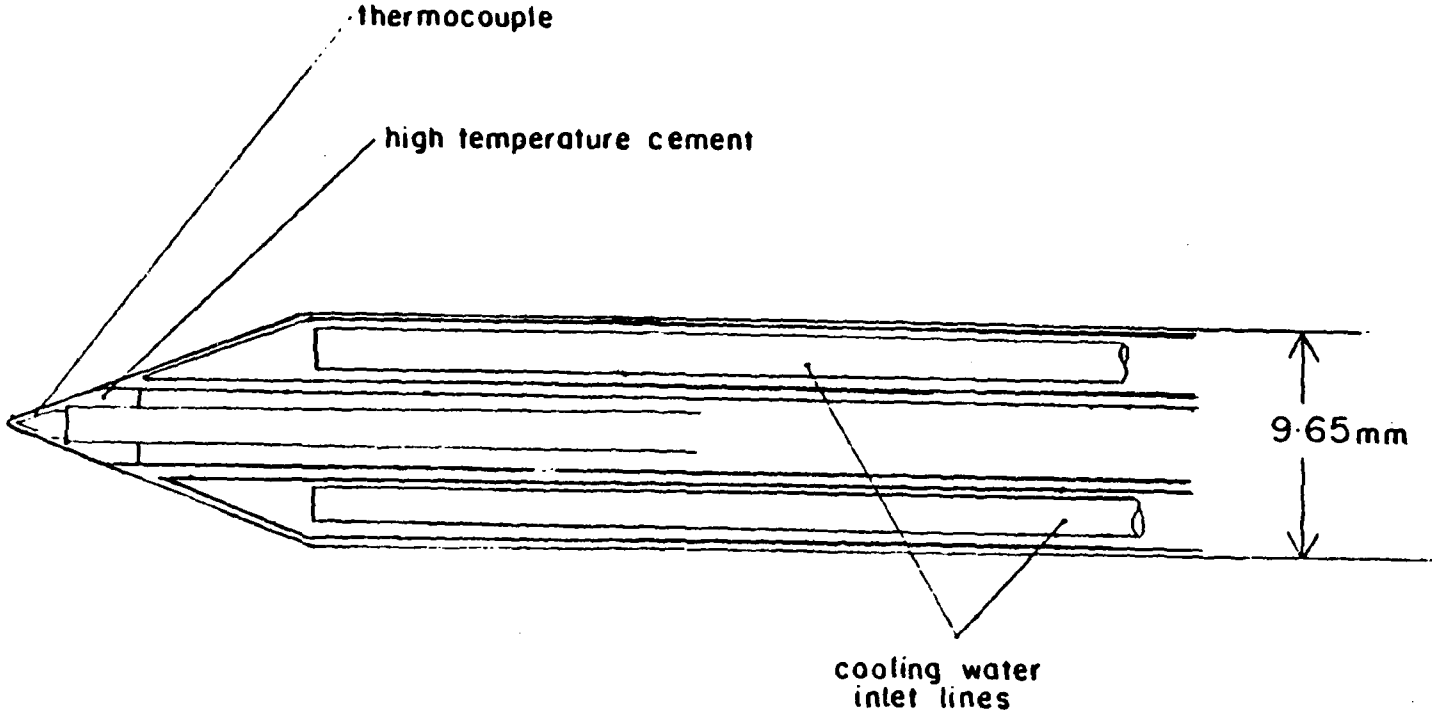

Figure 27. Schematic of Modified Temperature Probe.

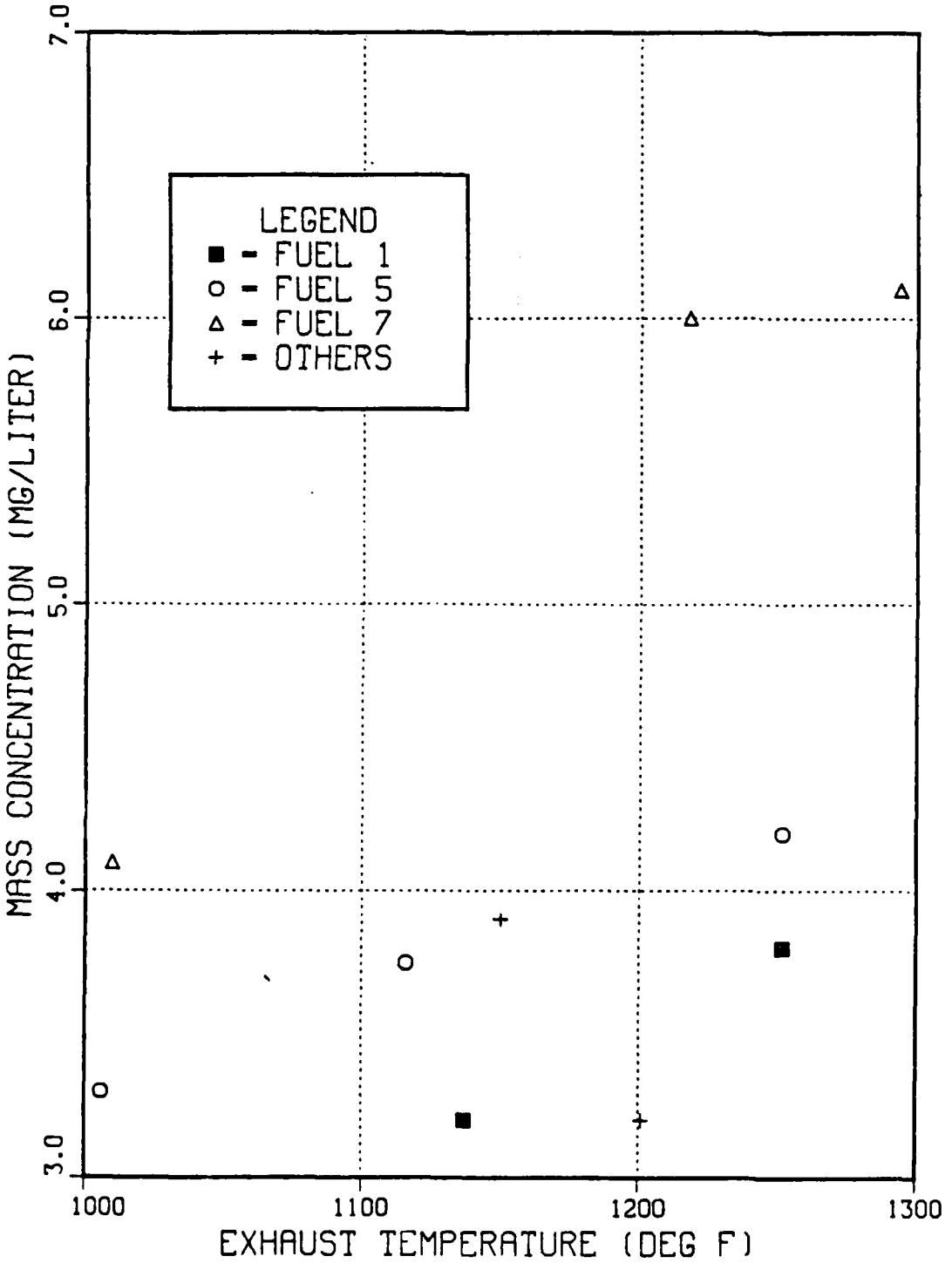

Figure 26. Mass Concentration vs. Exhaust Temperature.

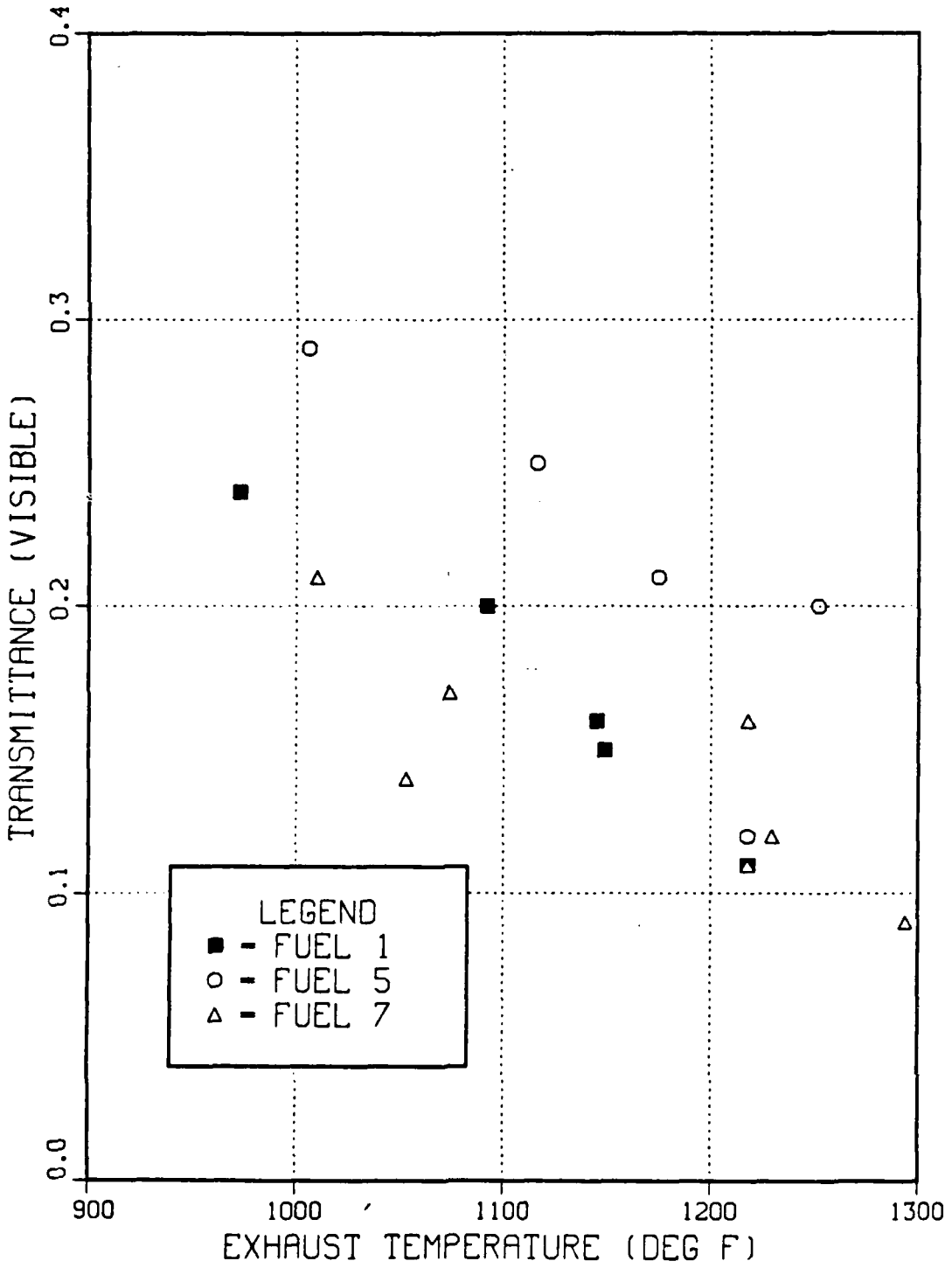

Figure 25. Visible Transmittance vs. Exhaust Temperature

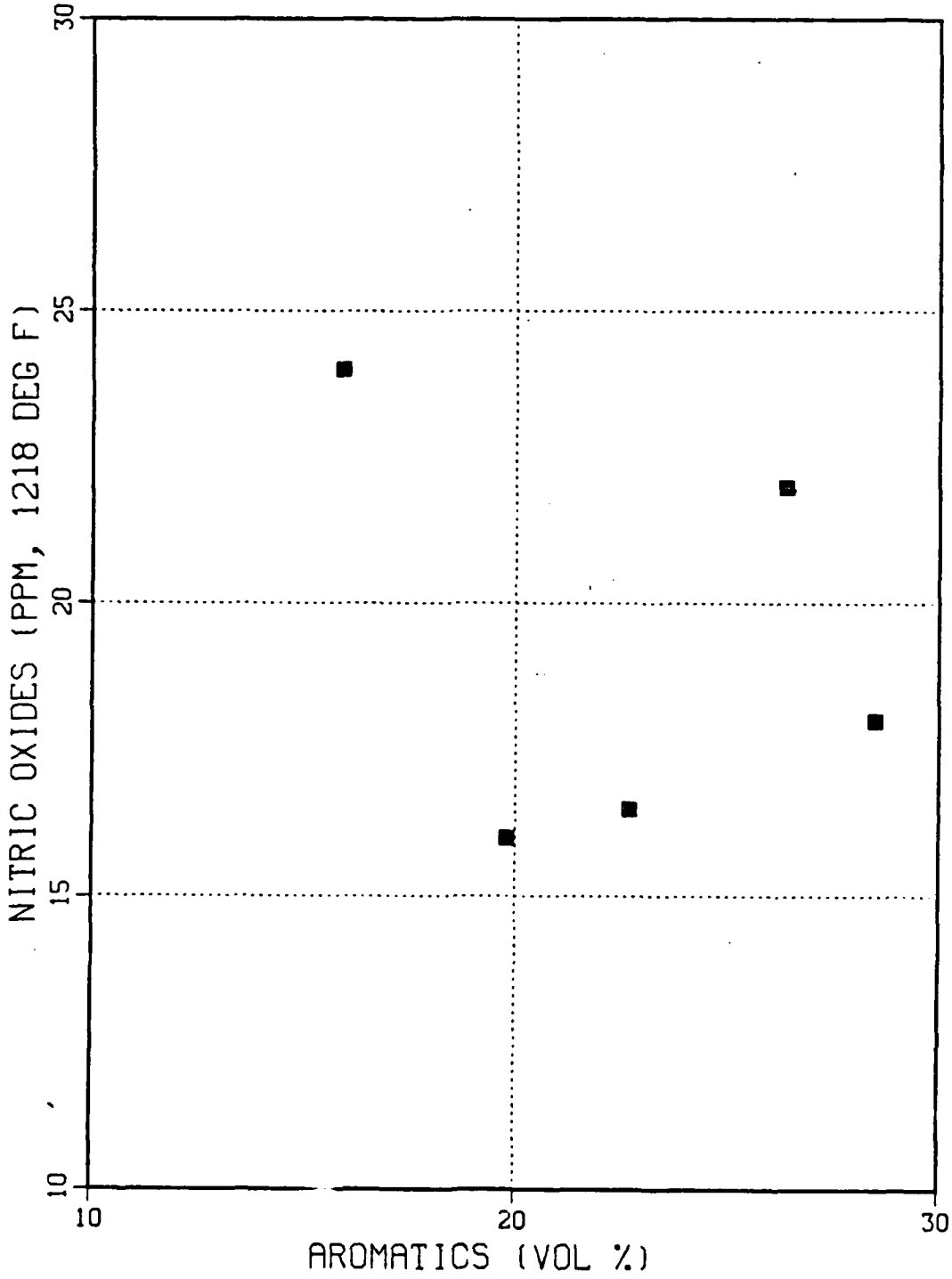

Figure 24. Nitric Oxides vs. Aromatics.

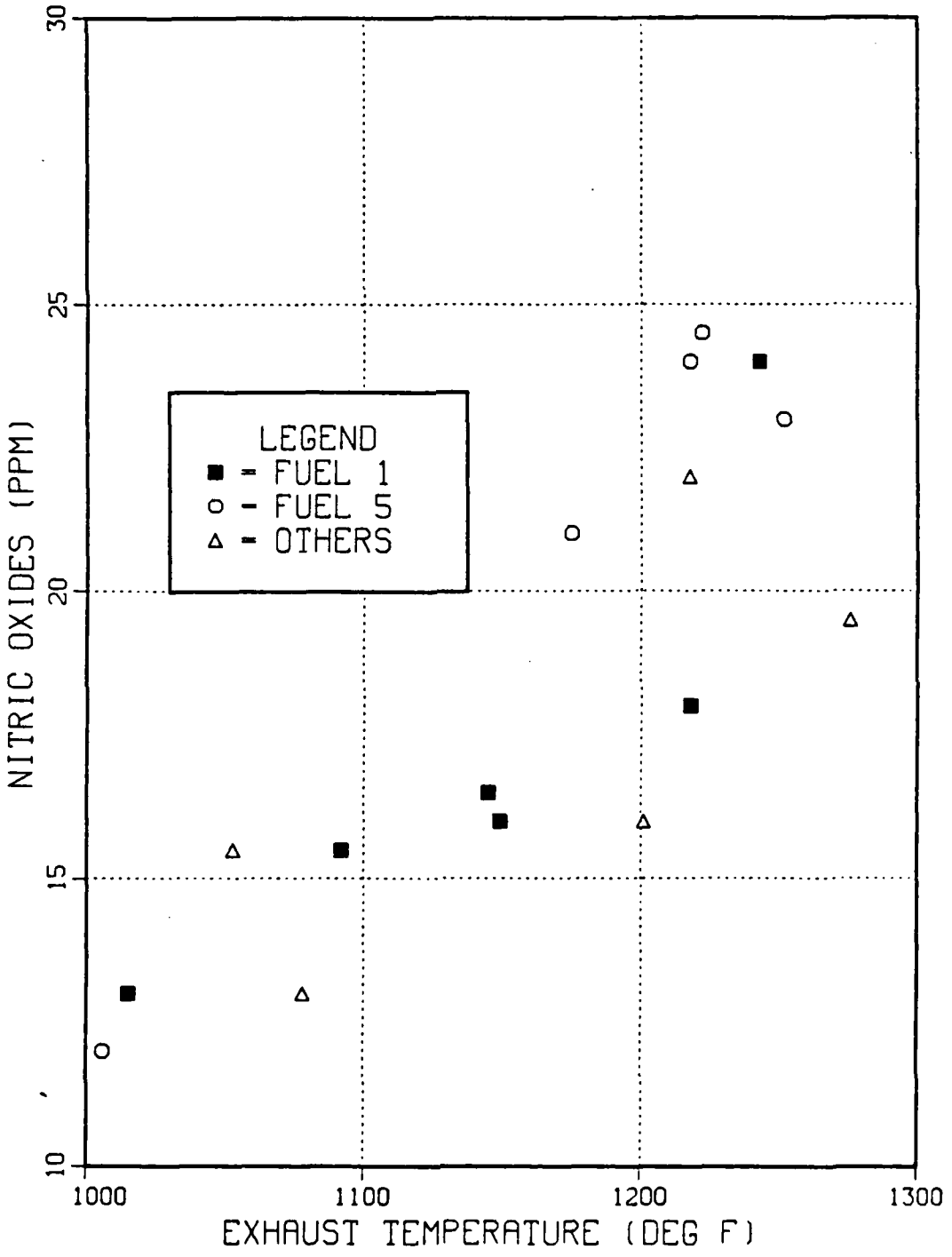

Figure 23. Nitric Oxides vs. Exhaust Temperature

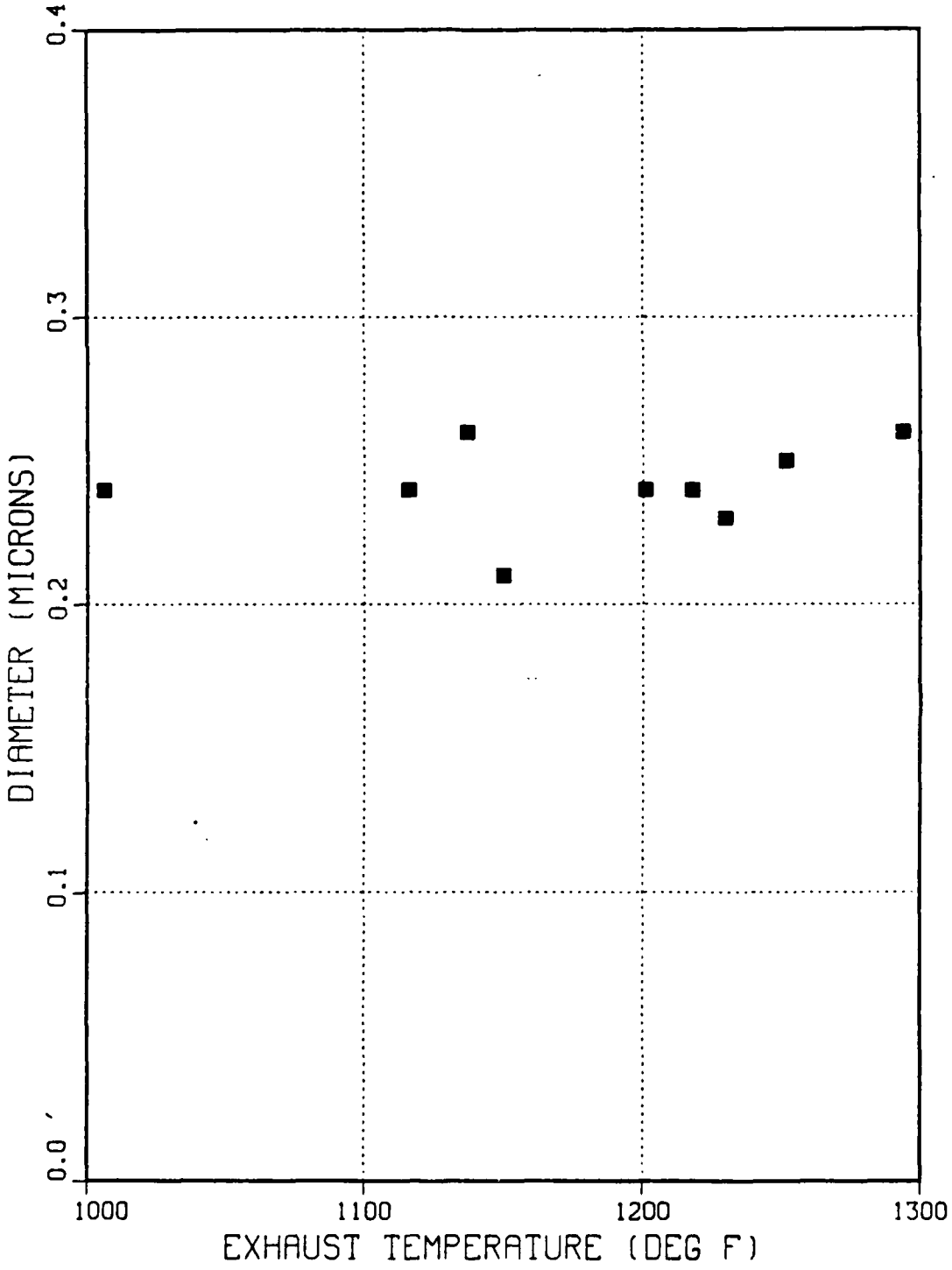

Figure 22. Particle Size vs. Exhaust Temperature

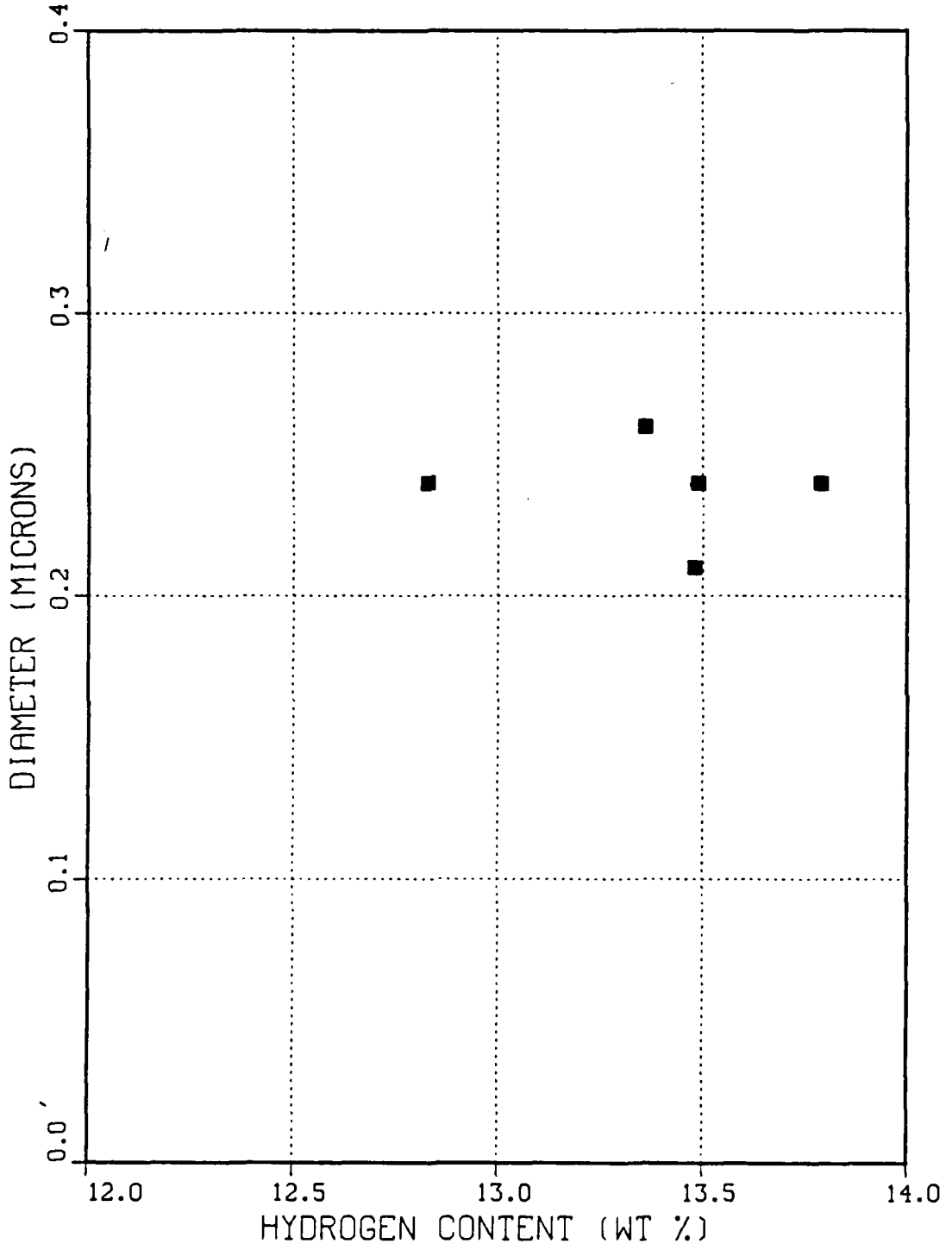

Figure 21. Particle Size vs. Hydrogen Content

Figure 35. SEM Photograph, 8.0μm Filter, Run D

Figure 36. SEM Photograph, 0.2μm Filter, Run D

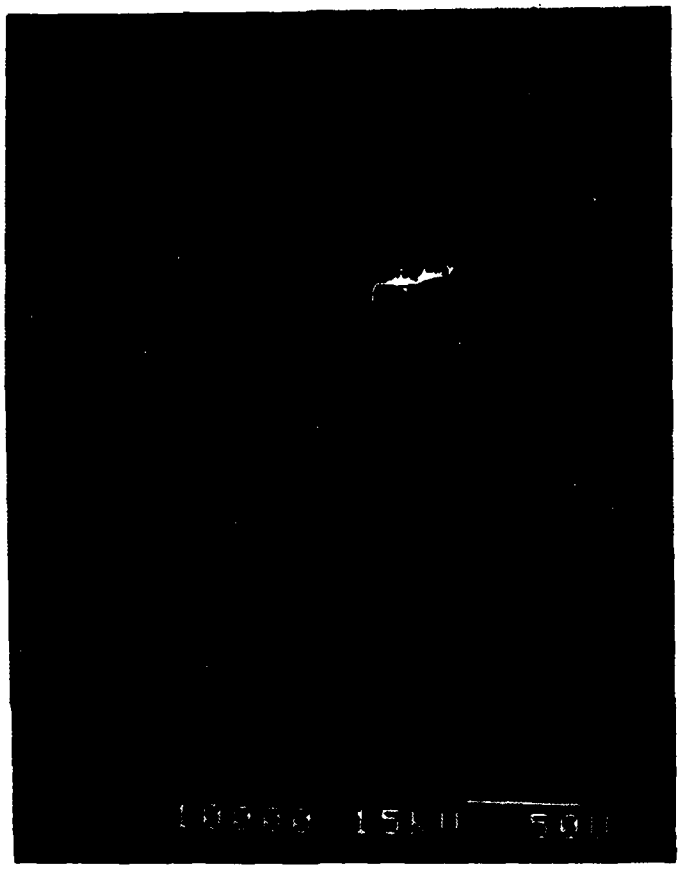

Figure 37. SEM Photograph, 8.0μm Filter, Run A, Low Magnification

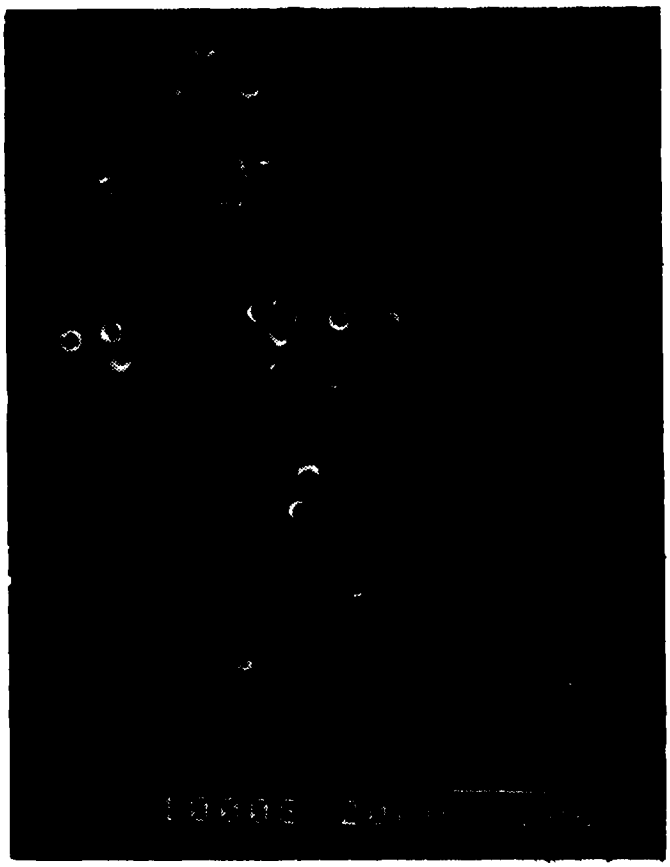

Figure 38. SEM Photograph, 8.0um Filter, Run D, Low Magnification

LIST OF REFERENCES

1. Naval Air Propulsion Test Center, Report No. NAPTC-PE-103, Evaluation of Smoke Suppressant Fuel Additives for Jet Engine Test Cell Smoke Abatement, by A. F. Klarman, February 1977.

2. Naval Air Propulsion Test Center, Evaluation of the Extended Use of Ferrocene for Test Cell Smoke Abatement; Engine and Environmental Test Results, by A. F. Klarman, October 1971.

3. Naval Postgraduate School Report No. NPS-67-82-004, An Investigation of the Effects of Smoke Suppressant Fuel Additives on Engine and Test Cell Exhaust Gas Opacities, by D. W. Thornburg, T. R. Darnell, D. W. Netzer, May 1982.

4. Naval Postgraduate School Report No. NPS-67-82-13, An Investigation of the Effectiveness of Smoke Suppressant Fuel Additives for Turbojet Applications, by J. R. Bramer, D. W. Netzer, September 1982

5. Oller, T. I., Gleason, C. C., Kenworthy, M. J., Cohen, J. D., and Barh, D. W., Fuel Mainburner/Turbine Effects, General Electric Company, AFWAL-TR-2100, May 1982.

6. Naval Air Propulsion Center Interim Report LR-84-2, Effects of Fuel Properties on T63-A-5A Engine Smoke and Gaseous Emissions Levels, by J. J. Zidzik, 23 January 1984.

7. Cashdollar, K. I., Lee, C. K., and Singer, J. M., "Three Wavelength Light Transmission Technique to Measure Smoke Particle Size and Concentration", Applied Optics, Vol 18, No. 11, June 1979, pp. 1763-1769

8. Dobbins, R. A., and Jizmagian, G. S., "Optical Scattering Cross Sections for Polydispersions of Dielectric Spheres", Journal of the Optical Society of America, Vol 56, No. 10, October 1966, pp. 1345-1354.

9. Samuelson, G. S., Hach, R. L., Poon, C. C., Bachalo, W. D., An Exploratory Study of Soot Sample Integrity and Probe Perturbation in a Swirl-Combustor, The American Society of Mechanical Engineers (ASME), PREPRINT No. 81-GT-27, 345 East 47th Street, New York, New York 1981.

10. Rosfjord, T. J., "Influence of Fuel Chemical Properties on Gas Turbine Combustors", Assessment of Alternative Aircraft Fuels, NASA Conference Publication 2307, November 1983, pp. 31-45.

11. Marx, M., T63 Cerium Test, NAPC Internal Memorandum, December 10, 1984.

12. Finch, III, S. P., "Prediction of Test Cell Visible Emissions", Air Force Civil Engineering Center Report, AFCEC-TR-76-47, Dec. 1976.

13. Devorkin, H., Chass, R. L., and Fudurich, A. P., Air Pollution Source Testing Manual, Air Pollution Control District--Lost Angeles CA, 1972.

INITIAL DISTRIBUTION LIST

	NO. OF COPIES
1. Library Code, 0142 Naval Postgraduate School Monterey, CA 93943	2
2. Department of Aeronautics Code 67 Naval Postgraduate School Monterey, CA 93943	
Chairman	1
D. W. Netzer	10
P. J. Hickey	2
3. Dean of Research Code 012 Naval Postgraduate School Monterey, CA 93943	1
4. Defense Technical Information Center Cameron Station Alexandria, VA 22314	2
5. Chief of Naval Operations Navy Department Washington, DC 20360 (Attn: Code OP451, IP453)	2
6. Chief of Naval Material Navy Department Washington, DC 20360 (Attn: Codes: 08T241, 044P1)	2
7. Commander Naval Air Systems Command Washington, DC 20361 (Codes: AIR-01B, 330D, 3407, 4147A, 50184, 5341B, 53645, 536B1)	8
8. Commanding Officer Naval Air Rework Facility Naval Air Station North Island San Diego, CA 92135 Code: 64270	1
9. Commander Naval Facilities Engineering Command 200 Stoval Street Alexandria, VA 22332 (Codes: 104, 032B)	2

10. Naval Construction Battalion Center — 3
Port Hueneme, CA 93043
(Codes: 25, 251, 252)

11. U. S. Naval Academy — 1
Annapolis, MD 21402
(Attn: Prof. J. Williams)

12. Arnold Engineering Development Center — 1
Arnold AFS, TN 37342
(Code: DYR)

13. Air Force Aero Propulsion Laboratory — 1
Wright-Patterson AFB, OH 45433
(Code: SFF)

14. Detachment 1 — 2
(Civil & Environmental Engineering
Division Office)
HQ ADTC (AFSC)
Tyndall AFB, FL 32401
(Code: EV, EVA)

15. Army Aviation Systems Command — 1
P. O. Box 209
St. Louis, MO 63166
(Code: EQP)

16. Eustis Directorate — 1
USA AMR & DL
Ft. Eustis, VA 23604
(Code: SAVDL-EU-TAP)

17. National Aeronautics and Space Admin. — 1
Lewis Research Center
2100 Brookpark Road
Cleveland, OH 44135
(Attn: Mail Stop 60-6 (R. Rudley))

18. Federal Aviation Administration — 1
National Aviation Facility Experimental Ctr.
Atlantic City, NJ 08405

19. Naval Air Propulsion Center — 3
Trenton, NJ 08628
(Code: PE 71:AFK)

20. Naval Ocean Support Center — 2
271 Catalina Boulevard
San Diego, CA 92152
(Attn: M. Lepor, M. Harris, Code 5121)

21. Naval Air Rework Facility — 1
Alameda, CA 94501
(Attn: G. Evans, Code 642)

END

FILMED

9-85

DTIC